Chapter I

Diluted magnetic semiconductor quantum dots

This chapter aim to present the system we will study as well as the main theoretical tools one needs to understand it fully. We begin presenting the semiconductors and their electronic structure, and how the strains affect it. We then reduce the dimensions of the system we look at to get to one of the core of this thesis: the quantum dot (QD). We first see how the confinement affect the carriers energies, and we then study the QD optical properties, detailing the effects of the carrier exchange interaction and the anisotropy of the strains in the QD on its emission.

In the next sections, we open the discussion on the magnetic atoms, starting with the Diluted Magnetic Semiconductors, semiconductors with a low density of magnetic impurity inserted in the lattice. We see how these impurities can dramatically change the behaviour of the carriers and thus the properties of said semiconductor. We then give more details on the two atoms we focus on in this thesis: the Manganese and the Chromium. The second section details their interactions with the carriers, while we study in the third their interaction with the semiconductor crystal field.

Finally, we give a simple example of application for these theories, studying a simple system: an exciton and a single Manganese atom in a quantum dot.

I.1 II-VI semiconductor quantum dots

I.1.1 Band structure of CdTe/ZnTe

CdTe and ZnTe are two II-VI semiconductors, meaning they are composed of an anion from the column VI of periodic table (Te), and a cation from the column II (Cd or Zn). They both crystallize in a zinc blend structure when grown in Molec-

ular Beam Epitaxy (MBE, see Chap. ?? for more informations on this technique). As shown in Fig. I.1, in this structure, each species is organized in a face centred lattice, one them being shift from the other by a quarter of the [111] diagonal. Each ion is then in a tetragonal environment, meaning the zinc-blende structure is of the T_d space-group.

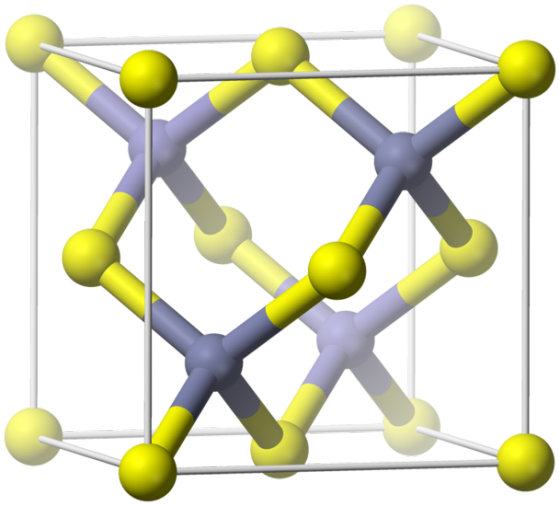

Figure I.1: Zinc-blende crystal elementary cell. Both CdTe and ZnTe crystallize in this structure.

The external orbitals are s for the cation ($4d^{10}5s^2$ for Cd, $3d^{10}4s^2$ for Zn) and p for the anion ($4d^{10}5s^25p^4$ for Te). Considering a N units crystal, it then contain 8N valence electrons, coming from the s and p levels of the ions. The s and p orbitals of these atoms hybridize to form 8 levels, 4 bonding and 4 anti-bonding.

The lowest band of the bonding levels, coming from s orbitals, will be filled by 2N valence electrons. 6N will be taken to fill the three bonding bands of higher energy, formed by the hybridization of p orbitals. Those bonding states form the valence band. At higher energy, the anti-bonding states form the conduction band. Since all the available electrons are used to fill the valence band, the conduction band is empty in the ground state. The lower energy band of the conduction band is formed by the anti-symmetric combination of the s orbitals. At higher energy, the anti-symmetric hybridization of p orbitals form three other bands.

The energy needed to promote one electron from the higher energy state of the valence band to the lower energy state of the conduction band is called the gap. In the ZnTe and CdTe cases, they are equal to $E_{g,ZnTe} = 2.40$ eV and $E_{g,CdTe} = 1.60$ eV at 5K [1]. It is possible to promote an electron from the valence band to the

conduction band by injecting in the semiconductor at least as much energy as the size of the gap. This absence of an electron in the valence band can be viewed as a quasi-particle called a hole, with a spin and a charge opposed to the one of the promoted electron.

Introducing the spin-orbit interaction, the conduction band, formed by the hybridization of s orbitals, is of Γ_6 (spherical) symmetry at the center of the Brillouin zone (for $k \simeq 0$), two-fold degenerated, with an orbital momentum (spin) $\sigma = \frac{1}{2}$. In a similar fashion, the valence band will be split into two bands: a first one of Γ_8 symmetry, with a spin $J = \frac{3}{2}$, four-fold degenerated ; and the second one, at lower energy, of Γ_7 symmetry, with a spin $\frac{1}{2}$, two-fold degenerated. The splitting $\Gamma_7 - \Gamma_8$ is of $\Delta_{SO} \simeq 0.9$ eV in II-VI semiconductor. This gap is wide enough to ignore the effect of the Γ_7 band for the rest of this document and focusing on the effect between the top of the valence band and the bottom of the conduction band.

Since the conduction band has a spin $\frac{1}{2}$, we can write it using Pauli matrix, defining the following operators:

$$\sigma_x = \frac{1}{2}\begin{pmatrix} 0 & 1 \\ 1 & 0 \end{pmatrix} \quad ; \quad \sigma_y = \frac{1}{2}\begin{pmatrix} 0 & -i \\ i & 0 \end{pmatrix} \quad ; \quad \sigma_z = \frac{1}{2}\begin{pmatrix} 1 & 0 \\ 0 & -1 \end{pmatrix} \tag{I.1}$$

In the same fashion, we can define the spin operators in the top of the valence band. For spin a $\frac{3}{2}$, we have:

$$J_x = \begin{pmatrix} 0 & \frac{\sqrt{3}}{2} & 0 & 0 \\ \frac{\sqrt{3}}{2} & 0 & 1 & 0 \\ 0 & 1 & 0 & \frac{\sqrt{3}}{2} \\ 0 & 0 & \frac{\sqrt{3}}{2} & 0 \end{pmatrix} \quad ; \quad J_y = \begin{pmatrix} 0 & -\frac{i\sqrt{3}}{2} & 0 & 0 \\ \frac{i\sqrt{3}}{2} & 0 & -i & 0 \\ 0 & i & 0 & -\frac{i\sqrt{3}}{2} \\ 0 & 0 & \frac{i\sqrt{3}}{2} & 0 \end{pmatrix}$$
$$J_z = \begin{pmatrix} \frac{3}{2} & 0 & 0 & 0 \\ 0 & \frac{1}{2} & 0 & 0 \\ 0 & 0 & -\frac{1}{2} & 0 \\ 0 & 0 & 0 & -\frac{3}{2} \end{pmatrix} \tag{I.2}$$

Finally, for any spin operator O ($O = \boldsymbol{\sigma}$, $\mathbf{J}$ or any other spin operator of this document), we can define the ladder operator, flipping the considered spin by one unit, such as $O_+|O\rangle \propto |O+1\rangle$ and $O_-|O\rangle \propto |O-1\rangle$. They write in the general case as:

$$O_+ = O_x + iO_y \tag{I.3}$$
$$O_- = O_x - iO_y \tag{I.4}$$

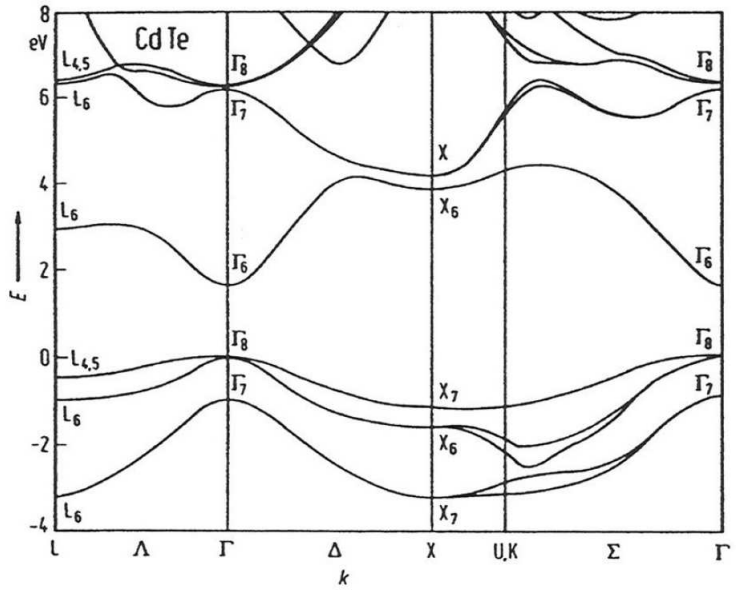

Figure I.2: CdTe band structure

The whole CdTe band structure is presented on Fig. I.2. One can note that CdTe is a direct gap semiconductor: the highest energy point of the valence band correspond to the lowest energy point of the conduction band, in Γ. Near the band edge, we can describe the curvature of the energy $E(\mathbf{k})$ of the band using an effective mass for the carrier on it:

$$E_{\{c,v\}}(\mathbf{k}) = -\frac{(\hbar k)^2}{2m_{\{c,v\}}(\mathbf{k})} \tag{I.5}$$

As we move away from the Γ point, the valence band into split two branches: the one with small curvature, meaning a high effective mass for the carriers on it, is called the heavy-hole (hh) band, while the one presenting the highest curvature and smallest effective mass is called the light-hole (lh) band.

One way to understand this evolution is to apply the **k.p** approximation, as proposed by Kane in 1957 [2]. This model gives an estimation of the electronic band structure starting from the exact solution and energy of the Schrödinger equation at the center of the Brillouin. The hamiltonian to resolve is then :

$$\left(\frac{p^2}{2m_0} + U(\mathbf{r})\right)|\psi_{n,\mathbf{k}}\rangle = E_{n,\mathbf{k}}|\psi_{n,\mathbf{k}}\rangle \tag{I.6}$$

with $U(\mathbf{r})$ the potential of the crystal, m_0 the mass of a free carrier and $|\psi_{n,\mathbf{k}}\rangle$ the Bloch wave, separated between a periodic part $u_{n,\mathbf{k}}(\mathbf{r})$ and plane-wave part

$\exp(i\mathbf{k}.\mathbf{r})$ as follow :

$$|\psi_{n,\mathbf{k}}\rangle = u_{n,\mathbf{k}}(\mathbf{r}) \exp(i\mathbf{k}.\mathbf{r}) \tag{I.7}$$

We solve this hamiltonian for carrier on the Γ_6 and Γ_8 bands. The z-axis is defined along the growth direction of the semiconductor and chosen as the quantization axis. The resolution was done in detail in Claire Le Gall PhD thesis [3]. We then find the energies:

$$\begin{aligned} E_c(k_z) &= E_c + \frac{\hbar^2 k_z^2}{2m_c} \\ E_{v,\pm\frac{1}{2}}(k_z) &= E_v - \frac{\hbar^2 k_z^2}{2m_{lh}} \\ E_{v,\pm\frac{3}{2}}(k_z) &= E_v + \frac{\hbar^2 k_z^2}{2m_0} \end{aligned} \tag{I.8}$$

with E_c (respectively, E_v) the energy of the conduction band (respectively, the valence band), m_c the effective mass of the carrier in the conduction band and m_{lh} the effective mass of the light hole. One can see that the splitting of the valence band separate the carrier with a spin $J_z = \pm\frac{3}{2}$ (hh) from the one with a spin $J_z = \pm\frac{1}{2}$ (lh). However, neglecting the bands other than Γ_6 and Γ_8 leads to a positive curvature for the hh. To correct this problem, we would have to take into account higher energies conduction bands, which will repel the hh band and give it its negative curvature.

Another solution to have the matrix describing the Γ_8 band is to use symmetry consideration. Luttinger showed in 1956 [4] that the only Hamiltonian fulfilling the cubic symmetry is:

$$\mathcal{H}_L = -\frac{h^2}{2m_0}\left(\gamma_1 k^2 I_4 - 2\gamma_2 \sum_i k_i^2 \left(J_i^2 - \frac{1}{3}J^2\right) - 2\gamma_3(k_x k_y (J_x J_y + J_y J_x) + c.p.)\right) \tag{I.9}$$

with γ_1, γ_2 and γ_3 the Luttinger parameters, I_4 the 4×4 identity matrix, $\mathbf{k}$ a vector of the Brillouin zone, $\mathbf{J}$ the orbital momentum operator with J_x, J_y and J_z being 4×4 matric satisfying $[J_x, J_y] = iJ_z$ and circular permutation ($c.p$). This hamiltonian can be simplified using the parameters:

$$\begin{aligned} A &= \gamma_1 + \frac{5}{2}\gamma_2 \\ B &= 2\gamma_2 \\ C &= 2(\gamma_3 - \gamma_2) \end{aligned} \tag{I.10}$$

	CdTe	ZnTe
E_g	1606 meV	2391 meV
ε_r	10.6	9.7
a_0	6.48 Å	6.10 Å
Δ_{SO}	0.90 eV	0.91 eV
γ_1	4.8	4.07
γ_2	1.5	0.78
γ_3	1.9	1.59
$m_{hh,z}$	0.556	0.398
$m_{hh,\perp}$	0.159	0.206
$m_{lh,z}$	0.128	0.178
$m_{lh,\perp}$	0.303	0.303
m_e	0.096	0.116

Table I.1: Physical parameters for CdTe and ZnTe.

The Luttinger hamiltonian can then be rewritten:

$$\mathcal{H}_L = -\frac{h^2}{2m_0}(Ak^2 I_4 - B(\mathbf{k}.\mathbf{J})^2 + C(k_x k_y (J_x J_y + J_y J_x) + c.p.)) \tag{I.11}$$

The B-term lifts the degeneracy of the Γ_8 band into two sub-bands as shown above, and is invariant under arbitrary rotations. The C-term describes the warping of the valence band.

In the spherical approximation, the Luttinger hamiltonian has two eigenvalues, giving us the value of the lh and hh effective mass:

$$\begin{aligned} E_{hh} &= -\frac{\hbar^2 k^2}{2m_0(A-2.25B)^{-1}} = -\frac{\hbar^2 k^2}{2m_0(\gamma_1 - 2\gamma_2)^{-1}} = -\frac{\hbar^2 k^2}{2m_{hh}} \\ E_{lh} &= -\frac{\hbar^2 k^2}{2m_0(A-0.25B)^{-1}} = -\frac{\hbar^2 k^2}{2m_0(\gamma_1 + 2\gamma_2)^{-1}} = -\frac{\hbar^2 k^2}{2m_{lh}} \end{aligned} \tag{I.12}$$

As expected from the band structure, the hh presents a negative curvature.

The parameters and carriers effective masses are given in the Tab. I.1.1.

The Luttinger hamiltonian is usually written in matrix form. In the $(u_{\Gamma_8,+\frac{3}{2}},$

$u_{\Gamma_8,+\frac{1}{2}}$, $u_{\Gamma_8,-\frac{1}{2}}$, $u_{\Gamma_8,-\frac{3}{2}}$) basis, we can rewrite it:

$$\mathcal{H}_L = -\frac{\hbar^2}{2m_0}\begin{pmatrix} a_{hh} & b_{Lutt} & c_{Lutt} & 0 \\ b^*_{Lutt} & a_{lh} & 0 & c_{Lutt} \\ c^*_{Lutt} & 0 & a_{lh} & -b_{Lutt} \\ 0 & c^*_{Lutt} & -b^*_{Lutt} & a_{hh} \end{pmatrix} \tag{I.13}$$

with:

$$\begin{aligned} a_{hh} &= (\gamma_1 - 2\gamma_2)k_z^2 + (\gamma_1 + \gamma_2)k_\parallel^2 \\ a_{lh} &= (\gamma_1 + 2\gamma_2)k_z^2 + (\gamma_1 - \gamma_2)k_\parallel^2 \\ b_{Lutt} &= -2\sqrt{3}\gamma_3(k_x - ik_y)k_z \\ c_{Lutt} &= -\sqrt{3}(\gamma_2(k_x^2 - k_y^2) - 2i\gamma_3 k_x k_y) \end{aligned}$$

I.1.2 Lattice mismatch and the Bir-Pikus Hamiltonian

ZnTe crystal has a lattice parameter of $a_{ZnTe} = 6.10$ Å, while CdTe one is of $a_{CdTe} = 6.48$ Å. This lattice mismatch results in stress in a CdTe layer grown on a ZnTe substrate:

$$\varepsilon_\parallel = \frac{a_{ZnTe} - a_{CdTe}}{a_{CdTe}} = -5.8\% \tag{I.14}$$

In order to represent this strain and see its effects on the bands, we need to define a hamiltonian representing them. Strains deform the structure, so let's begin the representation with an volume $V = x\mathbf{u_x} + y\mathbf{u_y} + z\mathbf{u_z}$, with $(\mathbf{u_x}, \mathbf{u_y}, \mathbf{u_z})$ an orthonormal basis. This volume will transform into another one $V' = x\mathbf{u'_x} + y\mathbf{u'_y} + z\mathbf{u'_z}$, where:

$$\begin{aligned} \mathbf{u'_x} &= (1 + \varepsilon'_{xx})\mathbf{u_x} + \varepsilon'_{xy}\mathbf{u_y} + \varepsilon'_{xz}\mathbf{u_z} \\ \mathbf{u'_y} &= \varepsilon'_{yx}\mathbf{u_x} + (1 + \varepsilon'_{yy})\mathbf{u_y} + \varepsilon'_{yz}\mathbf{u_z} \\ \mathbf{u'_z} &= \varepsilon'_{zx}\mathbf{u_x} + \varepsilon'_{zy}\mathbf{u_y} + (1 + \varepsilon'_{zz})\mathbf{u_z} \end{aligned} \tag{I.15}$$

ε'_{ij} represents an expansion of the vector i in the direction j. They are small deformation of the lattice, so we choose $|\varepsilon'_{ij}| \ll 1$. Such transformation can be decomposed in a symmetric part, the strain tensor, and an antisymetric one. We note the strain tensor $\overline{\overline{\varepsilon}}$, defined such as:

$$\varepsilon_{ii} = \varepsilon'_{ii} \tag{I.16}$$

$$\varepsilon_{ij} = \frac{1}{2}\left(\varepsilon'_{ij} + \varepsilon'_{ji}\right) \tag{I.17}$$

In the linear regime, the strain tensor $\overline{\overline{\varepsilon}}$ is proportional to the stress tensor $\overline{\overline{\sigma}}$, where σ_{ij} describe a force parallel to i applied on a surface perpendicular to j. Therefore, σ_{ii} will describe an elongation or compression stress, while σ_{ij} $(i \neq j)$ represents a shear stress. Since these tensor are symmetric, we can reduce the number of coefficient from nine to six: σ_{xx}, σ_{yy}, σ_{zz}, $\sigma_{xy} = \sigma_{yx}$, $\sigma_{xz} = \sigma_{zx}$ and $\sigma_{yz} = \sigma_{zy}$. Therefore, in the linear regime and for a cubic crystal, we can write the Hooke's law:

$$\begin{bmatrix} \sigma_{xx} \\ \sigma_{yy} \\ \sigma_{zz} \\ \sigma_{xy} \\ \sigma_{xz} \\ \sigma_{yz} \end{bmatrix} = \begin{bmatrix} C_{11} & C_{12} & C_{12} & 0 & 0 & 0 \\ C_{12} & C_{11} & C_{12} & 0 & 0 & 0 \\ C_{12} & C_{12} & C_{11} & 0 & 0 & 0 \\ 0 & 0 & 0 & 2C_{44} & 0 & 0 \\ 0 & 0 & 0 & 0 & 2C_{44} & 0 \\ 0 & 0 & 0 & 0 & 0 & 2C_{44} \end{bmatrix} \begin{bmatrix} \varepsilon_{xx} \\ \varepsilon_{yy} \\ \varepsilon_{zz} \\ \varepsilon_{xy} \\ \varepsilon_{xz} \\ \varepsilon_{yz} \end{bmatrix} \tag{I.18}$$

Since x, y and z are physically equivalent, as well as xy, xz and yz, only two diagonal coefficient are needed, C_{11} and C_{44}. These coefficient coupling strains in a direction to a force in the same direction are obviously positives.

When the considered cube is compressed in one direction (e.g. $\varepsilon_{zz} < 0$), it will expand in the other direction in order to minimize elastic energy (ε_{xx}, $\varepsilon_{yy} > 0$ in the example). If we don't allow strain in these other directions ($\varepsilon_{xx} = \varepsilon_{yy} = 0$), a stress in the x and y directions had to be applied to keep the cube from expanding in these directions (σ_{xx}, $\sigma_{yy} < 0$ in the example). We can therefore physically expect $C_{12} > 0$.

The strain hamiltonian can be constructed noticing that the strain tensor $\overline{\overline{\varepsilon}}$ induces a shift in the bands energy, and that any ε_{ij} has the same symmetry as $k_i k_j$. The hamiltonian should then be formarly identical to the Luttinger hamiltonian. In the Γ_8 subspace, we can then use the Luttinger Hamiltonian, written in Eq. I.9, replacing the $k_i k_j$ by ε_{ij}. We obtain the Bir-Pikus Hamiltonian by replacing the γ_j parameters by the Bir-Pikus parameters a_ν, b_{BP} and d_{BP} [5]:

$$\mathcal{H}_{BP} = a_\nu \sum_i \varepsilon_{ii} + b_{BP} \sum_i \varepsilon_{ii} \left(J_i^2 - \frac{1}{3} J^2 \right) + \frac{2 d_{BP}}{\sqrt{3}} \sum_{i>j} \varepsilon_{ij} \{ J_i J_j \} \tag{I.19}$$

with $\varepsilon = Tr(\overline{\overline{\varepsilon}}) = \varepsilon_{xx} + \varepsilon_{yy} + \varepsilon_{zz}$ and $\{J_i J_j\} = \frac{1}{2}(J_i J_j + J_j J_i)$

The a_ν term, called the hydrostatic term, shifts the Γ_8 energy. The b_{BP} term represents the shear strain. In case of non-equal ε_{ii}, its effect is to lift up the two Γ_8 sub-bands as did a $k \neq 0$ in the Luttinger hamiltonian. The d_{BP} term, the pure shear strain (i.e ε_{ij} with $i \neq j$), has the same effect on the Γ_8 band.

One can notice that the Bir-Pikus hamiltonian is completely independant from $\mathbf{k}$, meaning that the band hamiltonian of a strain semiconductor is simply the sum

of the Luttinger hamiltonian $\mathcal{H}_L$ (Eq. I.9) and the Bir-Pikus hamiltonian $\mathcal{H}_{BP}$ (Eq. I.19).

Let see how this apply to a CdTe layer deposited on a ZnTe layer. As previously, we define z as the growth direction. As shown at the begin of this part, CdTe and ZnTe have a lattice mismatch of 5.8%. Since both crystallize in a cubic lattice, the strains are the same in the x and y direction. We can then write the strains in the xy plane:

$$\varepsilon_{xx} = \varepsilon_{yy} = \varepsilon_{\parallel} = \frac{a_{ZnTe} - a_{CdTe}}{a_{CdTe}} \tag{I.20}$$

In the z direction, however, no stress applies: the crystal is free to expand in this direction in order to reduce the elastic energy. Therefore, we can write $\sigma_{zz} = 0$ and, according to Hooke's law in Eq. I.18:

$$\begin{aligned} \sigma_{zz} &= C_{12}\varepsilon_{xx} + C_{12}\varepsilon_{yy} + C_{11}\varepsilon_{zz} \\ &= 0 \end{aligned} \tag{I.21}$$

Using equality I.20, we can then deduce:

$$\varepsilon_{zz} = -\frac{2C_{12}}{C_{11}}\varepsilon_{\parallel} = -\frac{2C_{12}}{C_{11}}\frac{a_{ZnTe} - a_{CdTe}}{a_{CdTe}} \tag{I.22}$$

Since we grow CdTe over a ZnTe substrate, the CdTe lattice is compressed in the plane, i.e. $\varepsilon_{\parallel} < 0$. Since C_{11}, $C_{12} > 0$ and $\varepsilon_{\parallel} < 0$ for CdTe over ZnTe (see Eq. I.20), one can easily deduce that $\varepsilon_{zz} > 0$. In the hypothesis of no defect created by the lattice mismatch, all the other strain terms are equal to zero. We can then decompose this strain into two component: a hydrostatic part describing the volume variation without breaking the cubic symmetry, and a shear part introducing an anisotropy, breaking this symmetry:

$$\overline{\overline{\varepsilon_{hyd}}} = \frac{1}{3}(\varepsilon_{xx} + \varepsilon_{yy} + \varepsilon_{zz})I_3 \tag{I.23}$$

$$\overline{\overline{\varepsilon_{sh}}} = \overline{\overline{\varepsilon}} - \overline{\overline{\varepsilon_{hyd}}} \tag{I.24}$$

One can notice that $Tr(\overline{\overline{\varepsilon_{hyd}}}) = Tr(\overline{\overline{\varepsilon}}) = \varepsilon$. Since in the case of a hydrostatic compression, such as what is the case with CdTe over ZnTe, $\varepsilon_{hyd} < 0$, we then have $\varepsilon < 0$ and, according to the Bir-Pikus hamiltonian (Eq. I.19), the gap of CdTe increase. For CdTe, Bir-Pikus parameter are $a_\nu = 0.91$ eV, $b_{BP} = 0.99$ eV and $d_{BP} = 2.76$ eV [6].

Seeing that $\varepsilon_{ij} = 0$ for $i \neq j$, we can rewrite the Bir-Pikus hamiltonian without the shear strain term. Moreover, since $J^2 = J_x^2 + J_y^2 + J_z^2$ and that $\varepsilon_{xx} = \varepsilon_{yy} = \varepsilon_{\parallel}$, we can simplify this hamiltonian to:

$$\mathcal{H}_{BP,biax} = a_\nu \varepsilon I_4 + \frac{b_{BP}}{3}(\varepsilon_{\parallel} - \varepsilon_{zz})(J_x^2 + J_y^2 - 2J_z^2) \tag{I.25}$$

And, since we are in the valence band with $J = \frac{3}{2}$ and $J_x^2 + J_y^2 + J_z^2 = J(J+1)I_4$, we can simplify the Bir-Pikus hamiltonian to its final form in the case of biaxal strain:

$$\mathcal{H}_{BP,biax} = \left(a_\nu \varepsilon + \frac{5}{4} b_{BP}(\varepsilon_\parallel - \varepsilon_{zz})\right) I_4 - b_{BP}(\varepsilon_\parallel - \varepsilon_{zz}) J_z^2 \tag{I.26}$$

Using Eq. I.20 and I.22, we can easily calculate $\varepsilon_\parallel - \varepsilon_{zz}$. Since $J_z|n\rangle = n|n\rangle$, we find:

$$\begin{aligned} E_{\pm\frac{3}{2}} - E_{\pm\frac{1}{2}} &= -2b_{BP}\left(1 + \frac{2C_{12}}{C_{11}}\right)\frac{a_{ZnTe} - a_{CdTe}}{a_{CdTe}} \\ &= 2b_{BP}\left(1 + \frac{2C_{12}}{C_{11}}\right)\frac{a_{CdTe} - a_{ZnTe}}{a_{CdTe}} \end{aligned} \tag{I.27}$$

We find that, in a fully strained CdTe layer over a ZnTe substrate, the hh band is 300 meV above the lh one. In first approximation, we can then neglect the lh contribution in these nanostructures.

I.1.3 3D confinement: the quantum dot

Embedding a semiconductor in another one of larger gap creates trap for carriers, confining them in one or multiple directions. CdTe conduction band is at a lower energy than ZnTe ones, creating such a trap. Using the procedure described in Chap. **??**, we can create nanometre size island of CdTe in a ZnTe lattice, effectively confining electrons in all three directions, acting like a 3D trap for the free carriers. This lead to a quantization of the carriers energy levels and a discretization of the optical properties. This confinement being analogue to the Coulomb interaction of an isolated atom, such a structure is often dubbed "artificial atom". However, the interaction between the hole and the electron cannot be overlook, adding to this potential the Coulomb interaction between the particule and the quasi-particule. It consists of an attractive term, shifting energy levels, and an exchange interaction (discussed in Sec. I.1.4). Moreover, the hole being the absence of an electron, its energy, charge, spin, orbital momentum, $\mathbf{k}$ and mass are, by definition, opposite to the missing electron. The electron-hole system has a hydrogen-like behaviour and is called an exciton.

Before studying in more detail the exchange interaction between the hole and the electron, we will see the optical properties of this system. In order to do so, we develop the carrier wave-function on all the Bloch states:

$$\Psi(\mathbf{r}) = \sum_{n,\mathbf{k}} c_{n,\mathbf{k}} \psi_{n,\mathbf{k}} = \sum_{n,\mathbf{k}} c_{n,\mathbf{k}} u_{n,\mathbf{k}}(\mathbf{r}) \exp(i\mathbf{k}.\mathbf{r}) \tag{I.28}$$

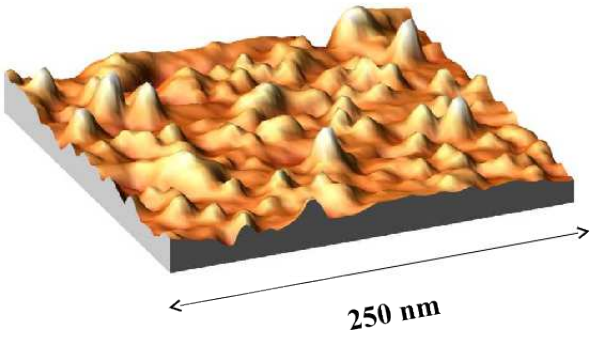

Figure I.3: AFM image (AFM image (250 nm × 250 nm) of CdTe/ZnTe quantum dots before caping. The dot density is estimated to be in the 10^{10} dots.cm^{-2} range.

Since we are in a confined environment, we can consider only the states around $\mathbf{k} = 0$. Since we consider the band extrema, we neglect for this part the inter-band wave function mixing and use the effective-mass approximation. We can then limit the expansion of Bloch state to an expansion on the $u_{n,0}(\mathbf{r})\exp(i\mathbf{k}.\mathbf{r})$, with $n = \Gamma_6$ for the conduction band and $n = \Gamma_8$ for the valence. We can then write:

$$\Psi_c(\mathbf{r}) \simeq \sum_{\mathbf{k}} c_{\mathbf{k}} u_{\Gamma_6,0}(\mathbf{r})\exp(i\mathbf{k}.\mathbf{r}) = F_e(\mathbf{r})u_{\Gamma_6,0} \tag{I.29}$$

$$\Psi_v(\mathbf{r}) \simeq \sum_{J_z=\{\pm\frac{3}{2},\pm\frac{1}{2}\},k} c_{J_z,\mathbf{k}} u_{\Gamma_8,J_z}(\mathbf{r})\exp(i\mathbf{k}.\mathbf{r}) = \sum_{J_z=\{\pm\frac{3}{2},\pm\frac{1}{2}\}} F_{J_z}(\mathbf{r})u_{\Gamma_8,J_z} \tag{I.30}$$

with $F_e(\mathbf{r}) = \sum_{\mathbf{k}} c_{\mathbf{k}}\exp(i\mathbf{k}.\mathbf{r})$ the electron envelop function and $F_{J_z}(\mathbf{r}) = c_{J_z,\mathbf{k}}\exp(i\mathbf{k}.\mathbf{r})$, $J_z = \{\pm\frac{3}{2},\pm\frac{1}{2}\}$ the hole envelop functions.

The effective mass approximation allows us to replace the periodic crystal potential and the free-electron kinetic energy by the effective Hamiltonian representing the band extrema, using m_e for the conduction band and $\mathcal{H}_L + \mathcal{H}_{BP}$ for the top of the valence band. Considering the effective mass is the same in CdTe and ZnTe, we can now work with the simple picture of an effective mass carrier with the envelop function defined in Eqs. I.29 and I.30, trapped in a potential $V_e(\mathbf{r})$ for the conduction band or $V_h(\mathbf{r})$ for the valence band, created by the band offset between the two semiconductors. We write the Schrödinger equations for these

particles:

$$\left(\frac{\hbar^2}{2m_e}\Delta\right) F_e(\mathbf{r}) + V_e(\mathbf{r})F_e(\mathbf{r}) = E_e F_e(\mathbf{r}) \tag{I.31}$$

$$(\tilde{\mathcal{H}}_L + \tilde{\mathcal{H}}_{BP} + V_h(\mathbf{r})) \begin{pmatrix} F_{+\frac{3}{2}}(\mathbf{r}) \\ F_{+\frac{1}{2}}(\mathbf{r}) \\ F_{-\frac{1}{2}}(\mathbf{r}) \\ F_{-\frac{3}{2}}(\mathbf{r}) \end{pmatrix} = E_h \begin{pmatrix} F_{+\frac{3}{2}}(\mathbf{r}) \\ F_{+\frac{1}{2}}(\mathbf{r}) \\ F_{-\frac{1}{2}}(\mathbf{r}) \\ F_{-\frac{3}{2}}(\mathbf{r}) \end{pmatrix} \tag{I.32}$$

with $\tilde{\mathcal{H}}_L$ and $\tilde{\mathcal{H}}_{BP}$ the hole hamiltonians, opposite to the electron hamiltonians defined in Eq. I.9 and I.19. In $\tilde{\mathcal{H}}_L$, the k-terms transform into a gradient of the envelop function with the form $i\nabla$. For simplicity, the $\tilde{}$ will be dropped in the next equations. The derivation of the effective mass approximation can be found in reference [7].

As pointed out in the end of Sec. I.1.2, the gap between lh and hh is wide enough to neglect lh contribution in first approximation. This is called the heavy hole approximation, uncoupling the four differential equations defined in Eq. I.32. Only the ground states $|\pm\frac{3}{2}\rangle$ are considered, with the effective mass given by the diagonal term of $\mathcal{H}_L$, noted $m_{h,\parallel}$ in the plane and $m_{h,z}$ along the growth axis. The spin operator J_x, J_y and J_z can then be redefined in the heavy-hole space as j_x, j_y, j_z, written with the Pauli matrix looking like σ_x, σ_y and σ_z.

Even with those two approximations, this problem is still unsolvable analytically. However, it is possible for some chosen potentials. Let's consider a lens like quantum dot, with a radius in the xy plane, noted ρ, much larger than its height L_z. We can therefore define two different harmonic oscillators: a 2D oscillator $V_{c,v}(\rho)$ in the plane, and a 1D oscillator $V_{c,v}(z)$ along the growth axis:

$$V_{c,v}(\rho) = 4\Delta E_{c,v}\frac{\rho^2}{L_z^2} \tag{I.33}$$

$$V_{c,v}(z) = 4\Delta E_{c,v}\frac{z^2}{L_z^2} \tag{I.34}$$

with $\Delta E_{c,v}$ the difference of conduction (resp. valence) band energy between the two semiconductors. The potential of the whole quantum dot will the be $V_{c,v}(\mathbf{r}) = V_{c,v}(\rho)+V_{c,v}(z)$. Separating the potential in those two parts means we are searching for solution of the form $F(z,\rho,\theta) = \chi(z)\phi_{n,m}(\rho,\theta)$, with θ the angle between the position vector and the x axis.

We write the characteristic spatial width σ and characteristic frequency ω of

the 2D harmonic oscillator felt by the hole:

$$\Sigma_\rho^h = \sqrt{\frac{\hbar}{m_{h,\parallel}\omega_\rho^h}} \tag{I.35}$$

$$\omega_\rho^h = \sqrt{\frac{8\Delta E_v}{m_{h,\parallel}L_\rho^2}} \tag{I.36}$$

We can write the same equality along z replacing ρ by z and $m_{h,\parallel}$ by $m_{h,z}$. The same can be done for electron, replacing the $m_{h,\parallel}$ or $m_{h,z}$ by m_e and E_v by E_c.

We can find in textbook such as ref. [8] the solution of a harmonic oscillator from which we can deduce the solution for the ground state (GS) and the first two degenerated excited states. The first excited state is found to have an angular momentum $l_z = \pm 1$, and is then noted $Exc, \pm 1$. The envelop functions and energy are then found to be:

$$F_{c,v}^{GS}(z,\rho,\theta) = \frac{1}{(\sqrt{\pi}\Sigma_z)^{\frac{1}{2}}}\exp\left(-\frac{z^2}{2\Sigma_z^2}\right)\frac{1}{(\sqrt{\pi}\Sigma_\rho)^{\frac{1}{2}}}\exp\left(-\frac{\rho^2}{2\Sigma_\rho^2}\right) \tag{I.37}$$

$$E_{e,h}^{GS} = \hbar\frac{\omega_z^{e,h} + \omega_\rho^{e,h}}{2} \tag{I.38}$$

$$F_{c,v}^{Exc,\pm1}(z,\rho,\theta) = \frac{1}{(\sqrt{\pi}\Sigma_z)^{\frac{1}{2}}}\exp\left(-\frac{z^2}{2\Sigma_z^2}\right)\frac{1}{(\sqrt{\pi}\Sigma_\rho)^{\frac{1}{2}}}\exp\left(-\frac{\rho^2}{2\Sigma_\rho^2}\right)\frac{\rho}{\sigma_\rho}\exp(\pm i\theta) \tag{I.39}$$

$$E_{e,h}^{Exc,\pm1} = \hbar\frac{\omega_z^{e,h} + 3\omega_\rho^{e,h}}{2} \tag{I.40}$$

We see that these energy levels are quantified in a way looking like an isolated atom, as pointed earlier. In reference to the atomic notation, the ground state, lower energy level, is noted S and the two first degenerated level are noted P, even though atomic p-states usually are 3 fold degenerated.

One remarkable feature of the envelop functions is that both GS and the two first excited states present the same envelop along the z axis. The cause is directly the symmetry of the QD: since $L_z \ll L_\rho$, $\omega_z^{e,h} \gg \omega_\rho^{e,h}$, and since $E_{osc.\ harmo.} = (n+\frac{1}{2})\hbar\omega$, the next possible envelop function along the z axis is at higher energy than the next one in the plane. This geometry is also responsible for the 2 fold degeneracy of the P-states.

Both the GS and the excited states are once again degenerated due to the spin of the electron and the hole. The electron is in the conduction band with the Γ_6 symmetry: it can then take the value $\sigma_z = \pm\frac{1}{2}$ (noted $|\uparrow\rangle$ for $+\frac{1}{2}$ and $|\downarrow\rangle$ for $-\frac{1}{2}$). Since we are in the hh approximation, considering the lh are far enough from

the band edge to be negligible, the hole spin can only take the values $J_z = \pm\frac{3}{2}$ (noted $|\Uparrow\rangle$ for $+\frac{3}{2}$ and $|\Downarrow\rangle$ for $-\frac{3}{2}$). As pointed ahead, the hole is defined with the opposed characteristic of the missing electron (which may not be the one trapped in the QD). For instance, a hole $|\Downarrow\rangle$ corresponds to the absence of a valence electron $\Psi_v(\mathbf{r}) = u_{\Gamma_8,\frac{3}{2}}(\mathbf{r})F_{\frac{3}{2}}(\mathbf{r})$.

In order to find the optical properties of the quantum dot, we use the dipole approximation, giving the coupling to light as $H = -\frac{q}{m}\mathbf{p}.\mathbf{A}$, with $\mathbf{p}$ the momentum and $\mathbf{A}$ the vector potential. We can then determine the optical properties looking at the coupling through the $\mathbf{p}$ operator. In a QD, the light-matter interaction occur mainly through two processes: the absorption of a photon creating an exciton, and the recombination of an exciton emitting a photon. To model this, we consider the interband matrix element between the two electronic states Ψ_c and Ψ_v, as written in Eqs. I.29 and I.30:

$$|\langle\Psi_v|\mathbf{p}|\Psi_c\rangle|^2 = |\langle F_v|F_c\rangle|^2|\langle u_{\Gamma_8,J_z}|\mathbf{p}|u_{\Gamma_6,\sigma_z}\rangle|^2 \tag{I.41}$$

The first term is just the overlap of the envelop function, making sure the hole and the electron are of the right state: a transition between a P state of the valence band and a S state in the conduction band is then forbidden.

The second term, showing the interband matrix elements, depending only on the symmetry of the Bloch functions, will then draw the rule for the recombination. We use the notation define above to note the electron state in the conduction band. The valence band, formed by p atomic states, three times degenerated, can be written from the $|X\rangle$, $|Y\rangle$ and $|Z\rangle$ electronic states as follows:

$$|+1\rangle = -\frac{|X\rangle + i|Y\rangle}{\sqrt{2}} \tag{I.42}$$

$$|0\rangle = |Z\rangle \tag{I.43}$$

$$|-1\rangle = \frac{|X\rangle - i|Y\rangle}{\sqrt{2}} \tag{I.44}$$

We can now write the states of the conduction band by composing these electronic states to the spin states:

$$|u_{\Gamma_8,+\frac{3}{2}}\rangle = |+1\rangle|\uparrow\rangle \tag{I.45}$$

$$|u_{\Gamma_8,+\frac{1}{2}}\rangle = \sqrt{\frac{2}{3}}|0\rangle|\uparrow\rangle + \sqrt{\frac{1}{3}}|+1\rangle|\downarrow\rangle \tag{I.46}$$

$$|u_{\Gamma_8,-\frac{1}{2}}\rangle = \sqrt{\frac{2}{3}}|0\rangle|\downarrow\rangle + \sqrt{\frac{1}{3}}|-1\rangle|\uparrow\rangle \tag{I.47}$$

$$|u_{\Gamma_8,-\frac{3}{2}}\rangle = |-1\rangle|\downarrow\rangle \tag{I.48}$$

Since we are working in the hh approximation, we neglect the contribution of the states $|u_{\Gamma_8,\pm\frac{1}{2}}\rangle$, calculating the interband matrix element only for $|u_{\Gamma_8,\pm\frac{3}{2}}\rangle$. Since $|\uparrow\rangle$ and $|\downarrow\rangle$ are orthogonal states, it is then clear that there is only two optically active transitions:

- between $|u_{\Gamma_6,\uparrow}\rangle$ and $|u_{\Gamma_8,+\frac{3}{2}}\rangle$ (hole $|\Downarrow\rangle$), coupled by $p_- = p_x - ip_y$, corresponding to $\sigma-$ photon absorption or emission.
- between $|u_{\Gamma_6,\downarrow}\rangle$ and $|u_{\Gamma_8,-\frac{3}{2}}\rangle$ (hole $|\Uparrow\rangle$), coupled by $p_+ = p_x + ip_y$, corresponding to $\sigma+$ photon absorption or emission.

We see thus that, for an exciton in the S state of the QD, four configurations are possible. First, we have the bright states $|\uparrow\Downarrow\rangle$ for a $\sigma-$ absorption, with an angular momentum $X_z = \sigma_z + j_z = \frac{1}{2} - \frac{3}{2} = -1$; and $|\downarrow\Uparrow\rangle$, for a $\sigma+$ absorption, with an angular momentum $X_z = -\frac{1}{2} + \frac{3}{2} = +1$. Both of these states are optically active, meaning their transitions are permitted and they can recombine radiatively. Two other states, not able to recombine radiatively, can exists and are called dark states: $|\uparrow\Uparrow\rangle$, with an angular momentum $X_z = +2$, and $|\downarrow\Downarrow\rangle$, with an angular momentum $X_z = -2$.

Approximating the QD potential as harmonic usually overestimate the confinement, and thus the single-particle energy. But the wave-functions found in this chapter can still be used as trial wave-functions for variational calculations in other potential, in order to estimate the correct energy level.

We discussed in this chapter about the neutral exciton (X), formed by a single electron-hole pair. However, several types of exciton can be observed in a quantum dots. First to consider are the charged excitons. In this case, a supplementary charge is injected in the QD in addition to the exciton, forming a hole-hole-electron (X^+) or hole-electron-electron (X^-) complex. It also happen that two excitons with opposed spins are trapped in a dot. This complex is called biexciton, noted X^2, and relax to leave a single neutral exciton in the QD. Charged biexciton and other multi-exciton complex also exist but are not discussed in this thesis. Even if the physics of each of this systems is different, the selection rules devised in this chapter apply to all of them.

I.1.4 Electron-hole exchange in quantum dots

An electron in the conduction band of a semiconductor interacts with all the electrons of the valence band. Solving such a system would be impossible. However, as shown in [9], we can treat this interaction as an interaction between this given electron and the corresponding hole, with a direct term and an exchange one. As classically expected from an electric interaction between two opposite charges, the

direct Coulomb interaction is attractive and therefore lower the overall energy of the system.

Taking into account the symmetry of the crystal, Bir and Pikus demonstrated that the complete hamiltonian can be decomposed in two different components: For an electron and a hole in the same Brillouin zone, the short-range exchange interaction is to be considered. It can be written:

$$\mathcal{H}_{eh}^{sr} = I_{eh}^{sr}\boldsymbol{\sigma}.\mathbf{j} + \sum_{i=x,y,z} b_i^{exch}\sigma_i j_i^3 \tag{I.49}$$

The first term lift the degeneracy between exciton of total angular moment $X = 2$ and $X = 1$. The second one take into account the reduction of symmetry in a cubic lattice and gives the dark states a fine structure. This have never been observed experimentally in bulk semiconductor, but it is expected to be much smaller than the lift induced by I_{eh}^{sr}.
For carriers in different Brillouin-zone, the long-range exchange interaction have to be considered. It mixes the bright exciton states in an anisotropic potential, such as the one of a partially relaxed self assembled quantum dot. In the heavy hole exciton subspace ($X_z = |+2\rangle$, $|+1\rangle$, $|-1\rangle$, $|-2\rangle$), it can be written as:

$$\mathcal{H}_{eh}^{lr} = \begin{pmatrix} 0 & 0 & 0 & 0 \\ 0 & 0 & \frac{1}{2}\delta_2 \exp(-2i\phi_2) & 0 \\ 0 & \frac{1}{2}\delta_2 \exp(-2i\phi_2) & 0 & 0 \\ 0 & 0 & 0 & 0 \end{pmatrix} \tag{I.50}$$

with δ_2 the splitting of the bright exciton induced by the exchange interaction.

In a quantum dot, the confinement of the carrier leads to a better overlap of the wave function and thus greater exchange energies. The exchange interaction has to be taken into account in order to fully understand the optical properties of such dots. Writing $\mathbf{j} = (j_z, j_+, j_-)$ and $\boldsymbol{\sigma} = (\sigma_z, \sigma_+, \sigma_-)$, we can develop the exchange hamiltonian in a QD symmetry for a quantization axis along z:

$$\begin{aligned} \mathcal{H}_{e-h}^{exch,QD} &= 2\delta_0 J_z \sigma_z + \frac{\delta_1}{2}\left(\exp(2i\varphi_1) j_+\sigma_- - \exp(-2i\varphi_1) j_-\sigma_+\right) \\ &\quad + \frac{\delta_2}{2}\left(\exp(2i\varphi_1) j_+\sigma_+ + \exp(-2i\varphi_1) j_-\sigma_-\right) \end{aligned} \tag{I.51}$$

with δ_0 representing the splitting between dark and bright exciton, δ_1 the splitting between the bright exciton states and δ_2 the splitting between the dark exciton states. δ_0 value is controlled both by long-range and short-range interaction, and is typically of about 1 meV in CdTe/ZnTe. δ_1 only appear in anisotropic quantum dot and is induced by the long-range interaction, warying between a few tens and a few hundreds of μeV. Finally, δ_2 primarily arise from the short-range interaction.

We note φ_1 the direction of the strain anisotropy in the QD. Calculating the eigenstate of the hamiltonian I.54, we find the optically active states are linearly polarized along φ_1 and $\varphi_1 + 90°$ as followed:

$$|\pi_{\varphi_1}\rangle = \frac{1}{\sqrt{2}}\left(\exp(-i\varphi_1)|+1\rangle + \exp(i\varphi_1)|-1\rangle\right) \tag{I.52}$$

$$|\pi_{\varphi_1+90°}\rangle = \frac{1}{\sqrt{2}}\left(\exp(-i\varphi_1)|+1\rangle - \exp(i\varphi_1)|-1\rangle\right) \tag{I.53}$$

This model works well for quantum dots with an elongated lens shape, in the C_{2v} symmetry. However, more realistic self-assembled quantum dots have symmetries which can deviate quite substantially from the idealized shapes of circular or ellipsoidal lenses. For a C_s symmetry (truncated ellipsoidal lens), additional terms coupling the dark and the bright excitons have to be included in the electron-hole exchange Hamiltonian. Following Ref. [10], the general form of the electron-hole exchange Hamiltonian in the heavy-hole exciton basis for a low symmetry quantum dot (C_s) is

$$\mathcal{H}_{eh} = \frac{1}{2}\begin{pmatrix} \delta_0 & e^{-i\pi/4}\delta_{11} & e^{i\pi/4}\delta_{12} & \delta_2 \\ e^{i\pi/4}\delta_{11} & -\delta_0 & e^{-i\pi/2}\delta_1 & -e^{i\pi/4}\delta_{12} \\ e^{-i\pi/4}\delta_{12} & e^{i\pi/2}\delta_1 & -\delta_0 & -e^{-i\pi/4}\delta_{11} \\ \delta_2 & -e^{-i\pi/4}\delta_{12} & -e^{i\pi/4}\delta_{11} & \delta_0 \end{pmatrix} \tag{I.54}$$

I.1.5 Valence band mixing

The long range exchange interaction split the neutral exciton bright states in two linearly polarized lines, with a 90° angle between them. However, this simple picture doesn't fit well with the data, such as presented in Fig. I.4. For once, it is clear for the neutral species (X, X^2) that the angle between the polarization of the two lines is different from 90°. Moreover, the charged species (X^+, X^-) are found to present linear polarization dependency, when the presence of the second hole (X^+) or electron (X^-) with an opposite spin should compensate the exciton exchange interaction, and thus these system should not present any dependency in linear polarization.

In order to fully understand it dependency, we have to stop neglecting the light hole contribution. Looking at the general form of the Luttinger hamiltonian I.13, we see that it mixes heavy hole and light hole through its non-diagonal term b_{Lutt} and c_{Lutt}. The Bir-Pikus hamiltonian I.19 presents the same symmetry and the same form as the Luttinger hamiltonian and thus also induces a coupling between the lh states and the hh states. In general, we can write the hamiltonian describing the influence of shape and strain on the valence structure in the ($|\frac{3}{2},+\frac{3}{2}\rangle$, $|\frac{3}{2},+\frac{1}{2}\rangle$,

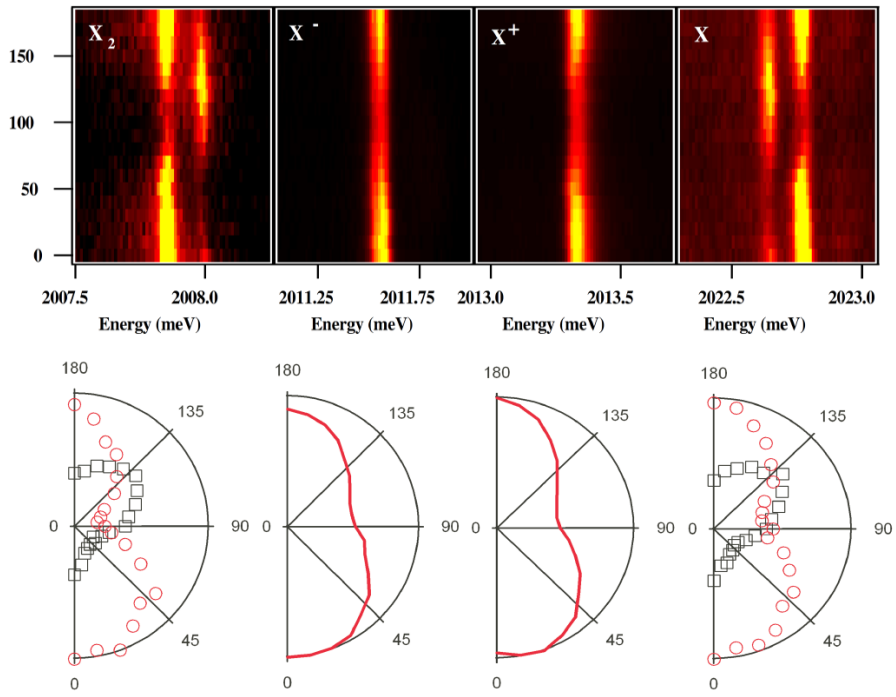

Figure I.4: PL intensities of the lines of the bi-exciton, the charged excitons and the neurtral exciton of CdTe/ZnTe quantum dot as the function of the angle of the linearly polarized detection. To simplify the reading, the intensities were also plotted on polar graph (bottom). Picture taken from Yoan Léger PhD thesis [11].

$|\frac{3}{2},-\frac{1}{2}\rangle$, $|\frac{3}{2},-\frac{3}{2}\rangle$) basis as:

$$\mathcal{H}_{VBM} = \begin{pmatrix} 0 & -Q & R & 0 \\ -Q^* & \Delta_{lh} & 0 & R \\ R^* & 0 & \Delta_{lh} & Q \\ 0 & R^* & Q^* & 0 \end{pmatrix} \tag{I.55}$$

where $R = \delta_{xx,yy} - i\delta_{xy}$ describes the mixing induced by an anisotropy in the QD xy plane, $Q = \delta_{xz} - i\delta_{yz}$ stands for an asymmetry in the plane containing the QD growth axis z, and Δ_{lh} is the splitting between lh and hh induced by the in-plane bi-axial strain and the confinement. The asymmetry described by Q may come from the QD shape or the strain distribution. This hh/lh mixing is called Valence Band Mixing (VBM).

Supposing a VBM only caused by strain anisotropy, through the Bir-Pikus hamiltonian, we can write the parameters as function of the Bir-Pikus parameters

and the crystal deformation ε_{ij} $(i,j = x,\, y,\, z)$ with x the (100) axis of the crystal lattice and z as defined above. The VBM parameters then writes as follow [12]:

$$\Delta_{lh} = 2b_{BP}\left(\frac{\varepsilon_{xx}+\varepsilon_{yy}}{2} - \varepsilon_{zz}\right) \tag{I.56}$$

$$R = id_{BP}\varepsilon_{xy} - b_{BP}\frac{\sqrt{3}}{2}(\varepsilon_{xx}-\varepsilon_{yy}) \tag{I.57}$$

$$Q = -\frac{2d_{BP}}{\sqrt{2}}(\varepsilon_{zx} - i\varepsilon_{zy}) \tag{I.58}$$

If we now suppose a system with pure in-plane strain anisotropy ($Q = 0$), for an origin of the energy at the top of the valence band, i.e. the hh band, we can rewrite the VBM hamiltonian in the same basis as above as:

$$\mathcal{H}_{VBM}^{in\ plane} = \begin{pmatrix} 0 & 0 & \rho_s\exp(-2i\theta_s) & 0 \\ 0 & \Delta_{lh} & 0 & \rho_s\exp(-2i\theta_s) \\ \rho_s\exp(2i\theta_s) & 0 & \Delta_{lh} & 0 \\ 0 & \rho_s\exp(2i\theta_s) & 0 & 0 \end{pmatrix} \tag{I.59}$$

with ρ_s the strain coupling amplitude and θ_s the angle between axis of the strain induced anisotropy in the QD plane and the x axis. One can notice that in the case of pure in-plane anisotropy, $|+\frac{3}{2}\rangle$ only mixes with $|-\frac{1}{2}\rangle$ and $|-\frac{3}{2}\rangle$ with $|+\frac{1}{2}\rangle$. An anisotropy along the z axis, growth axis of the dots, is needed to mix $|\pm\frac{3}{2}\rangle$ with $|\mp\frac{1}{2}\rangle$. With this notation, in the limit of weak VBM, we can now rewrite the ground state of the holes as pseudo-spin in order to take the hh/lh mixing into account:

$$|\tilde{\Uparrow}\rangle \propto |+\frac{3}{2}\rangle - \frac{\rho_s}{\Delta_{lh}}\exp(2i\theta_s)|-\frac{1}{2}\rangle \tag{I.60}$$

$$|\tilde{\Downarrow}\rangle \propto |-\frac{3}{2}\rangle - \frac{\rho_s}{\Delta_{lh}}\exp(-2i\theta_s)|+\frac{1}{2}\rangle \tag{I.61}$$

And we have to define new angular momentum operator for these pseudo-spin:

$$\tilde{J}_+ = \frac{\rho_s}{\Delta_{lh}}\begin{pmatrix} 0 & -2\sqrt{3}\exp(-2i\theta_s) \\ 0 & 0 \end{pmatrix} \tag{I.62}$$

$$\tilde{J}_- = \frac{\rho_s}{\Delta_{lh}}\begin{pmatrix} 0 & 0 \\ -2\sqrt{3}\exp(2i\theta_s) & 0 \end{pmatrix} \tag{I.63}$$

$$\tilde{J}_s = \begin{pmatrix} \frac{3}{2} & 0 \\ 0 & -\frac{3}{2} \end{pmatrix} \tag{I.64}$$

$\tilde{J}_\pm$ are the ladder operators, flipping the hole spin, whereas $\tilde{J}_z$ return the spin value. This last operator confirm these states are mainly hh. This pseudo spin description is enough in most of the case to understand the effect of the VBM, and we will use it to study how it modify the emission of the quantum dot.

In order to do so, we begin to consider the emission of an charged state. Since, as explained earlier, the exchange interaction is null is such systems, it will allows us to focus only on the VBM effect. We can ignore the envelop function, testing mainly the overlap of the carriers wave function and thus not affecting the polarization of the emission. We write the polarization of the detection $\mathbf{e} = \cos(\alpha)\mathbf{e_x} + \sin(\alpha)\mathbf{e_y}$. We then can find the oscillator strength of the transition:

$$\begin{aligned} \Omega(\alpha) &\propto |\langle \uparrow | \cos(\alpha) p_X + \sin(\alpha) o_Y | \uparrow\downarrow \tilde{\Uparrow} \rangle|^2 \\ &= 1 + \frac{1}{3}\frac{\rho_s}{\Delta_{lh}}^2 + \frac{2}{\sqrt{3}}\frac{\rho_s}{\Delta_{lh}}\cos(2(\theta_s - \alpha)) \end{aligned} \tag{I.65}$$

with $\mathbf{p} = -i\hbar\boldsymbol{\nabla}$. Contrary to what is expected in the hh approximation, we see that the charged exciton can have a strong linear component, depending on the strength of the lh/hh mixing.

In the QD presented in Fig. I.4, the linear polarization rate $\rho_l = \dfrac{2A}{1+A^2} \approx 40\%$, with $A = \frac{\rho_s}{\sqrt{3}\Delta_{lh}}$ corresponding to a very strong lh-hh mixing, with $\frac{\rho_s}{\Delta_{lh}} \approx 0.75$. Experimentally, no correlation were found between the polarization axis of different QDs, even if they are close to each other, neither with the crystallographic axis. Such a behaviour can be explained considering the anisotropic relaxation of strains occurring during the growth of our QDs [13]. This behaviour was also observed in III-V compounds at low QD density (near the 2D-3D transition), also attributed to the effect of strains [14]. For the III-V system, this hypothesis is supported by AFM studies showing that, in such growth conditions, the dots are preferentially nucleating near structural defects [15]. In the case of II-VI materials, a strained induced hh/lh mixing us not surprising as the dislocation formation energy is lower [16].

For the charged states X^+ and X^-, only the VBM lead to this linear polarization, leading to the simple picture discussed in this section. However, in X and X^2, the VBM and the long range exchange interaction are in competition for the polarization of the emission. The strains tend to polarized it along θ_s and $\theta_s + 90°$, when the long range exchange interaction favour linear emission along φ_1 and $\varphi_1 + 90°$. This explains that the angle between the two linearly polarized exciton lines is not equal to 90°. Moreover, the valence band mixing results in a fine structure splitting through the short range exchange interaction that can either enhance or decrease the fine structure splitting due to the long range exchange interaction. In order to illustrate our point, we consider only the isotropic part of the short range exchange interaction between the electron and the light or heavy

hole:

$$\mathcal{H}_{eh}^{sr,iso} = I_{eh}\boldsymbol{\sigma}.\mathbf{J} \tag{I.66}$$

where $\frac{3}{2}I_{eh}$ corresponds to the energy splitting between bright and dark excitons due to the short range exchange interaction. The coupling between the bright states $|\downarrow \tilde{\Uparrow}\rangle$ and $|\uparrow \tilde{\Downarrow}\rangle$ through $\mathcal{H}_{eh}^{sr,iso}$ can be calculated using the pseudo-spin ladder operator defined in I.62 and I.63:

$$\langle\downarrow \tilde{\Uparrow}|\mathcal{H}_{eh}^{sr,iso}|\uparrow \tilde{\Downarrow}\rangle = \frac{1}{2\sqrt{3}}I_{eh}\frac{\rho_s}{\Delta_{lh}}\exp(-2i\theta_s) \tag{I.67}$$

Hence, the valence band mixing through the short range exchange interaction splits the bright states into two linearly polarized states along axis defined by the strain angle θ_s. The competition between this effect and the long range exchange interaction results in an angle between the two linearly polarized states different from 90°, as observed in the emission of CdTe/ZnTe QDs [17] and in InAs/GaAs ones [18]. Dark states are also coupled to each other in second order, giving them a weak oscillator strenght, with a dipole along z. A more in depth investigation of these effects was done in Yoan Léger PhD thesis [11].

I.2 Exchange interaction between carrier and magnetic atom

I.2.1 Exchange interaction in Diluted Magnetic Semiconductors

We looked until now at the structure of a so-called perfect semiconductor, without defect or impurity. However, we are interested in thesis to introduce a low density of either Manganese or Chromium atoms in the crystal, namely, impurities. A semiconductor doped in this fashion is called Diluted Magnetic Semiconductor (DMS). This magnetic atom will interact with the semiconductor electrons via its localized electrons on its exterior shell. For Mn and Cr, this orbital is the d orbital, so it will be the one considered in the following document. From the interactions between these electrons and the one in the conduction band of the semiconductor, new properties will arise. We will try in this chapter to write this interaction as a "Heisenberg" interaction:

$$\mathcal{H}_{Heisenberg} = I\boldsymbol{\sigma}.\mathbf{S} \tag{I.68}$$

with I the interaction constant, $\boldsymbol{\sigma}$ the electron spin and $\mathbf{S}$ the spin of the magnetic atom.

This formally simple interaction represents the Pauli exclusion principle through the interaction between two spins. Almost all the interactions in this chapter will be of this form, although presenting different physical processes, with only the interaction constant I varying from one another.

Both Cr and Mn are close in size to the Cd atoms they replace, so their insertion only induces a small perturbation in the crystal structure, meaning the semiconductor wave function will not be significantly altered by them. We can then as usual note the conduction electron wave function as $|\psi_{\mathbf{k}}\rangle|\sigma;\sigma_z\rangle \equiv |\psi_{\mathbf{k}};\sigma_z\rangle$, $|\psi_{\mathbf{k}}\rangle$ being the Bloch function of the semiconductor. On the other side, considering a magnetic atom at $\mathbf{r} = \mathbf{R_d}$, we write the spatial component of the wave function $\Phi_d(\mathbf{r} - \mathbf{R_d})$. Its total electronic spin, sum of the electron spins on its d orbital, is noted $|S;S_z\rangle$. The whole wave function of the magnetic atom is then $|\Phi_d;S_Z\rangle$.

Using Born-Oppenheimer approximation, we can write the hamiltonian for these electrons:

$$\mathcal{H}_{BO} = \sum_i \left(\frac{p_i^2}{2m_c} + V_c(\mathbf{r}_i) \right) + \frac{1}{2} \sum_{i,j} \frac{e^2}{4\pi\varepsilon_0 |\mathbf{r_i} - \mathbf{r_j}|} \tag{I.69}$$

The first term is a single particle hamiltonian, taking into account the kinetic energy of the electron and the crystal potential $V_c(\mathbf{r}_i)$ felt by the electron at the position $\mathbf{r}_i$. This potential includes the impurities' potential, meaning it will be different at the impurities positions rather than elsewhere in the semiconductor. The final term represents the Coulomb interaction between the electrons.

We can rewrite this hamiltonian using second quantification. We define the destruction (resp. creation) operator of a particle in the conduction band at the wave vector $\mathbf{k}$ and the spin σ as $a_{\mathbf{k},\sigma}$ (resp. $a^\dagger_{\mathbf{k},\sigma}$). In the same fashion, we define the destruction (resp. creation) operator of the electronic level of an impurity as $a_{d,S}$ (resp. $a^\dagger_{d,S}$). Supposing the number of electrons on the d orbital of the considered magnetic atom does not change, the hamiltonian I.69 then become:

$$\begin{aligned}\mathcal{H}_{SQ} &= \sum_{\mathbf{k},\sigma} E_{\mathbf{k}} a^\dagger_{\mathbf{k},\sigma} a_{\mathbf{k},\sigma} + \sum_S E_d a^\dagger_{d,S} a_{d,S} + \sum_{\mathbf{k},\mathbf{k'}} U_{\mathbf{k},\mathbf{k'}} a^\dagger_{\mathbf{k},\sigma} a_{\mathbf{k'},\sigma} \\ &\qquad + \sum_{\mathbf{k},\sigma,S} M_{\mathbf{k}} (a^\dagger_{\mathbf{k},\sigma} a_{d,S} + a^\dagger_{d,S} a_{\mathbf{k},\sigma}) + \frac{1}{2} \sum_{i,j,k,l} V_{i,j,m,n} a^\dagger_i a^\dagger_j a_n a_m \qquad \text{(I.70)} \\ &= \mathcal{H}_0 + \mathcal{H}_d + V_d + \mathcal{H}_{hyb} + \mathcal{H}_{Coulomb}\end{aligned}$$

The constant electron number supposition is good enough for the picture we want to draw since most of the spin-driven interactions do not induce a change of this number.

$\mathcal{H}_0$ represents the energy of the unperturbed wave function of the semiconductor, with E_k the energy of an electron with the wave vector $\mathbf{k}$.

$\mathcal{H}_d$ is the same as $\mathcal{H}_0$ but for an electron of the d orbital of the considered magnetic impurity, with E_d the energy of an electron on this orbital.

V_d represents the impurities potential, allowing the semiconductor electrons to scatter on it. However, Mn and Cr does not modify strongly the crystal potential. We can then consider that the states of the semiconductor $|\psi_k\rangle$ are also solution of the full crystal potential, including impurity, and neglect this term.

$\mathcal{H}_{hyb}$, also called the Anderson hamiltonian, mixes the semiconductor states with the states of the impurities. It represents an exchange interaction between an electron of the semiconductor and one of the d orbital of an impurity. We can write the exchange constant as:

$$V_{kd} = \int \mathrm{d}\mathbf{r}\psi_k^*(\mathbf{r})\mathcal{H}_1\Phi_d(\mathbf{r} - \mathbf{R_d}) \tag{I.71}$$

with $\mathcal{H}_1$ the one particle hamiltonian. This term depends on the Bloch state of both the semiconductor and the impurity, meaning it can be reduced to zero by the symmetry of such functions in some specific cases.

Let's now focus on last term, $\mathcal{H}_{Coulomb}$, representing the two particles exchange. i, j, m and n each represents a full wave function, both spatial and spin part, and can be either an electron of the semiconductor or of one of the impurities. We can then separate this hamiltonian in three different terms depending on the value of i, j, m and n and illustrated in Fig. I.5.

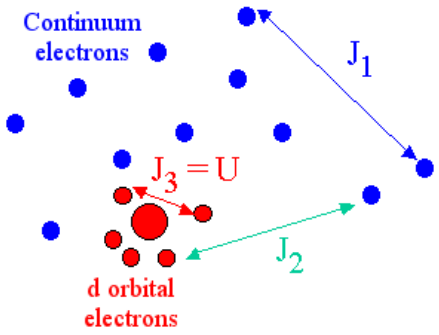

Figure I.5: Carrier interactions with no change of the number of electrons on the impurity, derived from the hamiltonian $\mathcal{H}_{Coulomb}$. Picture from Laurent Maingault PhD thesis [19].

We first consider two states belonging to the continuum, appearing as J_1 on the diagram. This is the hamiltonian H_{eh} introduced in Sec. I.1.4.

The next interaction we consider is the one of two electrons from a localized atom. It represents internal transitions of the atom, representing the Hund rule.

It is written:

$$\mathcal{H}_U = \sum_{d,S,S'} U a^\dagger_{d,S} a^\dagger_{d,S'} a_{d,S'} a_{d,S'} \tag{I.72}$$

with $U = \int \mathrm{d}\mathbf{r}\mathrm{d}\mathbf{r}' \frac{e^2}{4\pi\varepsilon_0|\mathbf{r}-\mathbf{r}'|}|\Phi_d(\mathbf{r})|^2|\Phi_d(\mathbf{r}')|^2$ the Coulomb interaction between two electrons on the same orbital with different spins. Thus, it costs more energy to add an electron on the same orbital than on another. We find back the Hund rule, with electrons first filing all orbitals with parallel spin before adding an electron to an orbital with another one, with opposed spin.

The third considered interaction is the one between an electron from the magnetic atom and an electron from the semiconductor. In the same fashion as with carriers of the bulk, it can be separated in two terms that will be developed in the next paragraphs: a direct Coulomb interaction between the two electrons, and an exchange interaction arising from the fermionic nature of electrons.

The direct Coulomb interaction doesn't depends on electrons spins. It only act on the total energy of the system and is therefore only needed when searching the total energy of an exciton. We write it:

$$K = + \sum_{\mathbf{k},\sigma,\sigma'} K_{\mathbf{k}} a^\dagger_{\mathbf{k},\sigma} a^\dagger_{d,\sigma'} a_{d,\sigma'} a_{\mathbf{k},\sigma} \tag{I.73}$$

with

$$K_k = \int \mathrm{d}\mathbf{r}\mathrm{d}\mathbf{r}' |\psi_k(\mathbf{r})|^2 \frac{e^2}{4\pi\varepsilon_0|\mathbf{r}'-\mathbf{r}|}|\Phi_d(\mathbf{r}')|^2$$

It is clear that the spin σ (resp. σ') of the k electron (resp. d electron) is not changed by this interaction. Since it only induce a shift in the total energy, we can redefine the origin of the energy axis to ignore it.

To go to the second term, the exchange interaction, we write it in second quantification:

$$J = + \sum_{k,k',\sigma,\sigma'} I^{ex}_{kk'} a^\dagger_{k',\sigma} a^\dagger_{d,\sigma'} a_{k,\sigma'} a_{d,\sigma} = + \sum_{k,k',\sigma,\sigma'} J_{kk'} a^\dagger_{k',\sigma} a_{k,\sigma'} a^\dagger_{d,\sigma'} a_{d,\sigma} \tag{I.74}$$

with

$$I^{ex}_{kk'} = \int \mathrm{d}\mathbf{r}\mathrm{d}\mathbf{r}' \psi^*_{k'}(\mathbf{r})\psi^*_k(\mathbf{r}') \frac{e^2}{4\pi\varepsilon_0|\mathbf{r}'-\mathbf{r}|} \Phi^*_d(\mathbf{r})\Phi^*_d(\mathbf{r}') \tag{I.75}$$

As can be sawn on Eq. I.74, this interaction exchange the spin σ and σ' of both electrons, thus its name. Eq. I.75 shows that the spin interaction comes from a Coulomb interaction between two fermions.

We define:

$$\begin{aligned}\sigma^z_{kk'} &= a^\dagger_{k,\sigma}a_{k',\sigma} - a^\dagger_{k,-\sigma}a_{k',-\sigma}\\ \sigma^+_{kk'} &= a^\dagger_{k,\sigma}a_{k',-\sigma}\\ \sigma^-_{kk'} &= a^\dagger_{k,-\sigma}a_{k',\sigma}\end{aligned} \tag{I.76}$$

Considering now that this interaction does not change the number of electrons on the d orbital of the considered magnetic atom, we can find the Kondo hamiltonian:

$$\mathcal{H}_{sd} = -\sum_{k,k'} I^{ex}_{kk'}\boldsymbol{\sigma}_{k,k'}.\mathbf{S} \tag{I.77}$$

Since $I^{ex}_{k,k'}$ is positive, the negative sign in front of the Kondo hamiltonian shows that the energy minimum is reached when the spins of both electrons are aligned, and is therefore ferromagnetic.

We can now write the hamiltonian I.70, detailing these new hamiltonians:

$$\mathcal{H}_{SQ} = \mathcal{H}_0 + \mathcal{H}_d + \mathcal{H}_{hyb} + \mathcal{H}_{eh} + \mathcal{H}_U + \mathcal{H}_{sd} \tag{I.78}$$

with the exchange constant in $\mathcal{H}_{hyb}$, $V_{kd} = \int \mathrm{d}\mathbf{r}\psi^*_k(\mathbf{r})\mathcal{H}_1\Phi_d(\mathbf{r}-\mathbf{R_d})$.

We now have two hamiltonians to model the exchange interaction between the impurities electrons and the one in the conduction band of the semiconductor: $\mathcal{H}_{hyb}$ and $\mathcal{H}_{sd}$. Schrieffer and Wolff rewrote the Anderson hamiltonian in order to give a form closer to the Kondo hamiltonian [20]:

$$\begin{aligned}\mathcal{H}_{hyb} &= \sum_{k,k'} V_{kd}V_{k'd}\left(\frac{1}{E_k-(E_d+U)} + \frac{1}{E_{k'}-(E_d+U)}\right.\\ &\qquad\left. -\frac{1}{E_k-E_d} - \frac{1}{E_{k'}-E_d}\right) a^\dagger_{k',\sigma}a_{k,-\sigma}a^\dagger_{d,S-2\sigma}a_{d,S}\\ &= \sum_{k,k'} I^{hyb}_{kk'}a^\dagger_{k',\sigma}a_{k,-\sigma}a^\dagger_{d,S-2\sigma}a_{d,S}\end{aligned} \tag{I.79}$$

The Fig. I.6 illustrates the different energies introduced in I.79, presenting virtual transitions to the d orbital of the magnetic atom. The two possible energies are E_d for the low energy level, and E_d+U for the high energy one, U being the energy needed to add an electron to the orbital.

Doing this transformation is an important step, since we are now able to use a Heisenberg type spin hamiltonian instead of a hamiltonian mixing wave functions, in addition to having the same formalism to write both type of exchange interactions, with just a difference in the exchange constants $I^{ex}_{kk'}$ and $I^{hyb}_{kk'}$.

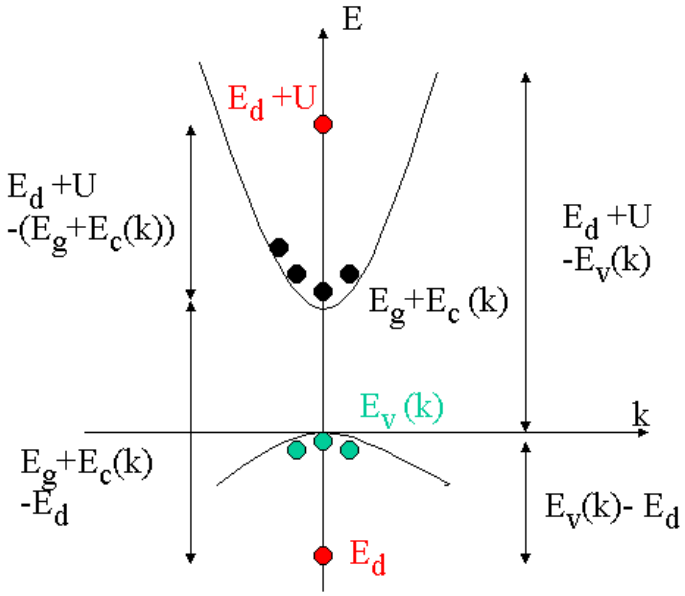

Figure I.6: Schema of the band structure and virtual transitions between valence band and conduction band. Picture from Laurent Maingault PhD thesis [19].

Supposing the coupling occurs between two electrons with a close k ($k \simeq k'$), we can rewrite $I^{hyb}_{kk'}$ as:

$$\begin{aligned} I^{hyb}_{kk'} &= 2|V_{kd}|^2 \frac{U}{(E_k - E_d)(E_k - (E_d + U)} \\ &= -2|V_{kd}|^2 \frac{U}{(E_k - E_d)(E_d + U - E_k)}) \end{aligned} \tag{I.80}$$

Looking ath the Fig. I.6, one can see that U and $E_k - E_d$ are both positive, while $E_k - (E_d + U)$ is negative. Thus, $I^{hyb}_{kk'}$ is negative, and we see that, while exchange leads to a ferromagnetic coupling, hybridization leads to an anti-ferromagnetic one. There will be a competition in the semiconductor between these two for every type of carrier.

Reusing the hypothesis done on Sec. I.2 of small k value, and the value of V_{kd} presented in Eq. I.71, we can rewrite the exchange constant:

$$I^{hyb}_{00,\{c,v\}} = -2 \left(\frac{U}{(E_{\{c,v\}}(0) - E_d)(E_d + U - E_{\{c,v\}}(0))} \right) \int \mathrm{d}\mathbf{r} \Phi^*_r(\mathbf{r}) \mathcal{H}_1 \psi^{\{c,v\}}_0 \tag{I.81}$$

$$I^{ex}_{00,\{c,v\}} = \int \mathrm{d}\mathbf{r}\mathrm{d}\mathbf{r}' \psi^{*\{c,v\}}_0(\mathbf{r}) \Psi^*_d \frac{e^2}{4\pi\varepsilon_0 |\mathbf{r}' - \mathbf{r}|} \psi^{\{c,v\}}_0(\mathbf{r}) \Psi_d \tag{I.82}$$

In the valence band, the semiconductor's atoms exterior orbitals have the p symmetry, as discussed in Sec. I.2. We then write I_{pd} as the sum of the hybridization and the exchange contributions:

$$I_{pd} = I^{hyb}_{00,v} + I^{ex}_{00,v} \tag{I.83}$$

In the conduction band, the orbitals are s, and so we will write the interaction I_{sd}. However, since s orbitals have a spherical symmetry, there is no hybridization contribution. The expression is then pretty easy:

$$I_{sd} = I^{ex}_{00,c} \tag{I.84}$$

Having define those, we can now rewrite the Hamiltonian of the interaction with one magnetic atom in the Heisenberg notation:

$$\begin{aligned} \mathcal{H}_{SQ} &= \mathcal{H}_0 + \mathcal{H}_{eh} + \underbrace{I_{sd}\boldsymbol{\sigma}.\mathbf{S}}_{\mathcal{H}_{sd}} + \underbrace{I_{pd}\mathbf{J}.\mathbf{S}}_{\mathcal{H}_{pd}} \\ &= \mathcal{H}_0 + \mathcal{H}_{eh} + \mathcal{H}_{sd} + \mathcal{H}_{pd} \end{aligned} \tag{I.85}$$

Since a DMS contain a small percentage of magnetic atoms, we can write the hamiltonian of the full semiconductor by summing on their positions. We finally get:

$$\mathcal{H}_{DMS} = \mathcal{H}_0 + \mathcal{H}_{eh} + \sum_i I_{sd}(\mathbf{R}_i)\boldsymbol{\sigma}.\mathbf{S}_i + \sum_i I_{pd}(\mathbf{R}_i)\mathbf{J}.\mathbf{S}_i \tag{I.86}$$

This can be further simplified with two approximations. First, since conduction electron sees a lot of different atomic sites, we can we can work with the mean value of the magnetic atoms spins, $\langle\mathbf{S}\rangle$, instead of their individual value $\mathbf{S}_i$. This is the mean field approximation, the magnetic atoms being seen as an effective magnetic field. And for the same reason, we can consider the electron interaction with each site of the crystal multiplied by the probability x of being occupied by a magnetic atom, instead of summing only on the magnetic atoms positions. This is the virtual crystal approximation. We can then rewrite:

$$\sum_i I_{sd}(\mathbf{R}_i)\boldsymbol{\sigma}.\mathbf{S}_i = x\sum_{\mathbf{R}} I_{sd}(\mathbf{R})\boldsymbol{\sigma}.\langle\mathbf{S}\rangle \tag{I.87}$$

Projecting along the quantization axis, we just replace $\boldsymbol{\sigma}.\langle\mathbf{S}\rangle$ by $\sigma_z\langle S_z\rangle$. Since the atoms are seen as a magnetic field, they induce a degeneracy lift ΔE_c between the two spin values of conduction electron, $|\sigma_z = \pm\frac{1}{2}\rangle$:

$$\Delta E_c = N_0 x\alpha\sigma_z\langle S_z\rangle \tag{I.88}$$

with $\alpha \propto I_{sd}^{00}$ the interaction constant between the impurity's and the conduction band's Bloch function at $\mathbf{k} = 0$, and N_0 the number of cell per volume.

The same consideration can be done for valence band. Hh and lh are separated via their spin values: $|J_z = \pm\frac{3}{2}\rangle$ for hh, $|J_z = \pm\frac{1}{2}\rangle$ for lh. We then get:

$$\Delta E_v = N_0 x \frac{\beta}{3} J_z \langle S_z \rangle \tag{I.89}$$

with $\beta \propto I_{pd}^{00}$ the impurity's and the valence band's Bloch function at $\mathbf{k} = 0$.

To be completely thorough with the analysis, we should also take into account the confinement due to the quantum dot. This means the wave vector $\mathbf{k}$ of the carriers can be different from 0, leading to small perturbative effect on $\mathcal{H}_{sd}$ and $\mathcal{H}_{pd}$. This was done thoroughly by Laurent Maingault in the Chap. I.3 of his PhD thesis [19]. It is shown that the hamiltonian changed as follow:

$$\begin{aligned}\mathcal{H}_{sd}(\mathbf{R}) = -\alpha \boldsymbol{\sigma}.\mathbf{S} \left| F_c(\mathbf{R}) - A_2 \left(\frac{\partial^2 F_c}{\partial z^2}(\mathbf{R}) + \frac{\partial^2 F_c}{\partial \rho^2}(\mathbf{R}) \right) \right|^2 \\ - \beta \boldsymbol{\sigma}.\mathbf{S} \left((C_2 - B_2) \left| \frac{\partial^2 F_c}{\partial z^2}(\mathbf{R}) \right|^2 + C_2 \left| \frac{\partial^2 F_c}{\partial \rho^2}(\mathbf{R}) \right|^2 \right)\end{aligned} \tag{I.90}$$

$$\mathcal{H}_{pd}(\mathbf{R}) = -\beta \mathbf{J}.\mathbf{S} |F_v(\mathbf{R}) - V_{kd} F_v''(\mathbf{R})|^2 \tag{I.91}$$

with $F_c(\mathbf{R})$ (resp. $F_v(\mathbf{R})$) the electron (resp. hole) envelop function, $F_v''(\mathbf{R})$ the second derivative of the hole envelop function, and A_2, B_2, C_2 constant depending on the semiconductor lattice. For CdTe, $A_2 = 10.3$ Å^{-2}, $B_2 = 0.781$ Å^{-2} and $C_2 = 19.8$ Å^{-2}.

I.2.2 Studied magnetic atoms: Mn and Cr

We will consider in the section the interaction between single magnetic atoms trapped in quantum dots and the carrier. Specifically, we will be interested in the interaction with a Manganese atom and with a Chromium atom. This does not change dramatically the picture we draw in the previous section. However, for the interaction between the semiconductor electrons and the magnetic atom d electrons, we will have to also take into account the overlap between the magnetic atom and the carriers. For a magnetic atom A, we then defined the exchange constant:

$$I_{eA} = \alpha |F_c(\mathbf{R})|^2 \tag{I.92}$$

$$I_{hA} = \beta |F_v(\mathbf{R})|^2 \tag{I.93}$$

Mn in CdTe

Using the exchange constant defined above, we can rewrite the hamiltonian I.85:

$$\begin{aligned} \mathcal{H}_{cMn} &= \mathcal{H}_{eMn} + \mathcal{H}_{hMn} \\ &= I_{eMn}\boldsymbol{\sigma}.\mathbf{S}_{Mn} + I_{hMn}\mathbf{J}.\mathbf{S}_{Mn} \end{aligned} \tag{I.94}$$

We ignore $\mathcal{H}_0$ here since it only shift the energy of the system without affecting the spins exchange interactions. In II-VI semiconductors, Mn is inserted as Mn^{2+}, with an electronic spin $S = \frac{5}{2}$. We can then write its spin operator as we did for the carrier in Sec. I.2:

$$S_{Mn,x} = \begin{pmatrix} 0 & \frac{\sqrt{5}}{2} & 0 & 0 & 0 & 0 \\ \frac{\sqrt{5}}{2} & 0 & \sqrt{2} & 0 & 0 & 0 \\ 0 & \sqrt{2} & 0 & \frac{3}{2} & 0 & 0 \\ 0 & 0 & \frac{3}{2} & 0 & \sqrt{2} & 0 \\ 0 & 0 & 0 & \sqrt{2} & 0 & \frac{\sqrt{5}}{2} \\ 0 & 0 & 0 & 0 & \frac{\sqrt{5}}{2} & 0 \end{pmatrix}$$

$$S_{Mn,y} = \begin{pmatrix} 0 & -\frac{i\sqrt{5}}{2} & 0 & 0 & 0 & 0 \\ \frac{\sqrt{5}}{2} & 0 & -i\sqrt{2} & 0 & 0 & 0 \\ 0 & \sqrt{2} & 0 & -\frac{3i}{2} & 0 & 0 \\ 0 & 0 & \frac{3}{2} & 0 & -i\sqrt{2} & 0 \\ 0 & 0 & 0 & \sqrt{2} & 0 & -\frac{i\sqrt{5}}{2} \\ 0 & 0 & 0 & 0 & \frac{\sqrt{5}}{2} & 0 \end{pmatrix} \tag{I.95}$$

$$S_{Mn,z} = \begin{pmatrix} \frac{5}{2} & 0 & 0 & 0 & 0 & 0 \\ 0 & \frac{3}{2} & 0 & 0 & 0 & 0 \\ 0 & 0 & \frac{1}{2} & 0 & 0 & 0 \\ 0 & 0 & 0 & -\frac{1}{2} & 0 & 0 \\ 0 & 0 & 0 & 0 & -\frac{3}{2} & 0 \\ 0 & 0 & 0 & 0 & 0 & -\frac{5}{2} \end{pmatrix}$$

In the conduction band, the electrons s orbitals are orthogonal to the d orbital of the Mn atom. No hybridization can then occur between these. Only the Coulomd interaction remain, leading to an overall ferromagnetic interaction between conduction band electrons and Mn electronic spin. Confirming this, $N_0\alpha = 0.22 \pm 0.01$ eV was measured [21].

The deduction is a bit harder to work out in the valence band. Valence electrons p orbitals are not orthogonal to Mn electrons d orbital, meaning there is a competition between the ferromagnetic Coulomb interaction and the anti-ferromagnetic

hybridization. However, the hybridization is usually stronger than Coulomb interaction for Mn in II-VI semiconductor, leading to an overall anti-ferromagnetic interaction between holes and Mn electronic spin [22]. For $Cd_xMn_{1-x}Te$, $N_0\beta = -0.88 \pm 0.01$ eV was measured, confirming this tendency [21].

Cr in CdTe

As for the Mn, we can rewrite the hamiltonian I.85 using the exchange interaction defined in the introduction of this section:

$$\begin{array}{rcccc} \mathcal{H}_{cCr} & = & \mathcal{H}_{eCr} & + & \mathcal{H}_{hCr} \\ & = & I_{eCr}\boldsymbol{\sigma}.\mathbf{S}_{Cr} & + & I_{hCr}\mathbf{J}.\mathbf{S}_{Cr} \end{array} \tag{I.96}$$

Once again, we ignore $\mathcal{H}_0$ since it didn't affect the spins exchange interaction. We can also write the Cr spin operators as follow:

$$\begin{aligned} S_{Cr,x} &= \begin{pmatrix} 0 & 1 & 0 & 0 & 0 \\ 1 & 0 & \sqrt{\frac{3}{2}} & 0 & 0 \\ 0 & \sqrt{\frac{3}{2}} & 0 & \sqrt{\frac{3}{2}} & 0 \\ 0 & 0 & \sqrt{\frac{3}{2}} & 0 & 1 \\ 0 & 0 & 0 & 1 & 0 \end{pmatrix} \\ S_{Cr,y} &= i \begin{pmatrix} 0 & -1 & 0 & 0 & 0 \\ 1 & 0 & -\sqrt{\frac{3}{2}} & 0 & 0 \\ 0 & \sqrt{\frac{3}{2}} & 0 & -\sqrt{\frac{3}{2}} & 0 \\ 0 & 0 & \sqrt{\frac{3}{2}} & 0 & -1 \\ 0 & 0 & 0 & 1 & 0 \end{pmatrix} \\ S_{Cr,z} &= \begin{pmatrix} 2 & 0 & 0 & 0 & 0 \\ 0 & 1 & 0 & 0 & 0 \\ 0 & 0 & 0 & 0 & 0 \\ 0 & 0 & 0 & -1 & 0 \\ 0 & 0 & 0 & 0 & -2 \end{pmatrix} \end{aligned} \tag{I.97}$$

For conduction band electrons, the situation is the same as with the Mn: the conduction electrons s orbital are orthogonal to the Chromium d orbital, and the hybridization is then null. Hence, only the Coulomb interaction remain and induce a ferromagnetic coupling between the electrons of the band and the Cr electronic spin. $N_0\alpha$ was never measured in $Cd_xCr_{1-x}Te$, but most most magnetic atoms

in II-VI semiconductor presents a value between 0.2 eV and 0.3 eV. It is then generally assume that, in II-VI semiconductor, $N_0\alpha \approx 0.2$ eV [23].

Once again, valence band is a bit more complicated: Coulomb interaction, leading a ferromagnetic coupling, competes with hybridization between valence band p electrons and Cr d electrons. Direct measure of $N_0\beta$ was neither done in $Cd_xCr_{1-x}Te$, so the competition between these two interactions is difficult to evaluate. Moreover, it has been showed that it was difficult to decide theoretically if the interaction between Cr and holes was ferromagnetic or anti-ferromagnetic both in CdTe and in ZnTe [24]. However, it was found that $N_0\beta$ was positive in $Cd_xCr_{1-x}S$ [25] and in most Zn based II-VI semiconductors, assuming $N_0\alpha = 0.2$ eV [22]. Especially, in ZnTe, still using this assumption, $N_0\beta = +3.6 \pm 1.2$ eV was found [23]. Since there is almost no valence band offset between ZnTe and CdTe, it seems safe to assume that $N_0\beta$ in CdTe is positive and thus the interaction between Cr and holes is ferromagnetic.

I.3 Fine and hyperfine structure of a magnetic atom in II-VI semiconductor

I.3.1 Mn atom in II-VI semiconductor

Mn is incorporated in II-VI semiconductors as Mn^{2+}. This ion is really weakly coupled to the strain state at its position. In first approximation, we can then consider it as an isolated ion occupying a cation site in the lattice. We will first study the free ion and then see the effect of the lattice on the different states.

The Mn^{2+} electronic structure $[Ar]3d^5$. Since the d orbital is five time degenerated (doubled when taking spin into account), it is half-full in the case of the Mn in II-VI. Following Hund's rule, the spin of those electron are all aligned, leading to an electron spin $S = \frac{5}{2}$ and, following Pauli exclusion principle ranging the electrons angular momenta from -2 to $+2$, an angular momentum $L = 0$.

We get from Hund's rule that adding an electron to an half-full orbital has a high energy cost. The lowest energy excited states are therefore the flipping of an electron. For a free atom, it leads to a first excited state with an angular moment $L = 4$. Following the spectroscopic notation of these states ${}^{(2S+1)}L$, the ground state is the noted ${}^6S$ ($L = 0$, $S = \frac{5}{2}$) and the first excited state is ${}^4G$ ($L = 4$, $S = \frac{3}{2}$). The flipping of one electron leads also to higher energy excited states, written in spectroscopic notation ${}^4P$, ${}^4D$ and ${}^4F$ in Fig. I.7.

Mn atom in inserted in the CdTe lattice replacing a Cd atom. The interaction with the crystal field will lift the degeneracies of the free atom level. Those new levels are written with the appropriate group theoritical transformation properties. The ${}^6S$ ground state is symmetrical and non-degenrated. Thus, in first order, it

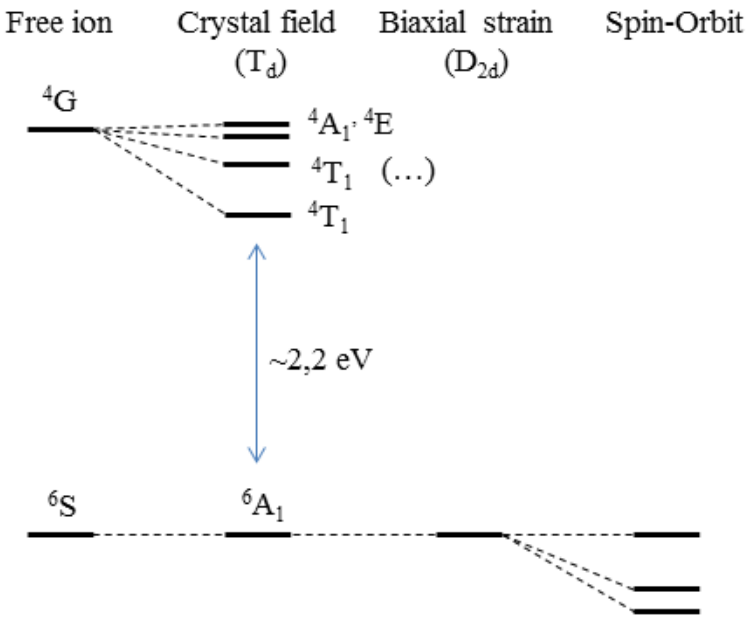

Figure I.7: A schematic diagram of the splitting of the lowest excited states of the $3d^5$ level (^{4}G) relative to the ground state (^{6}S) for a Mn^{2+} ion in the presence of a tetrahedral crystal field.

is not affected by the crystal field and is noted $^6A_1$. On the other hand, ^{4}G, the first excited state, is degenerated and therefore is affected by the crystal. It split into four different states: $^4T_1$, three-fold degenerated ; $^4T_2$, three-fold degenerated ; ^4E, two-fold degenerated ; and $^4A_1$, not degenerated. It has been shown by calculations that the effect of the crystal field is to pull the two ^{4}T levels closer to the ground state, while ^4E and $^4A_1$ are almost coincident and almost not affected by the crystal field [26–28]. Higher energy excited states would also be affected, but they are at high enough energy for their contribution not to be significant.

For a free atom, the transition between the ground state with $S = \frac{5}{2}$ and any of the excited state, with $S = \frac{3}{2}$ is forbidden by the $\Delta S = 0$ rule and the parity selection ones. However, in a II-VI lattice, the spin-orbit interaction and the absence of inversion symmetry relax those rules, and thus allow the transitions between $^6A_1$ and the different states coming from the ^{4}G splitting. $^6A_1 \rightarrow ^4T_1$ is the lowest energy of those transitions and therefore the most significant. It corresponds to approximately 2.2 eV. We saw in Sec. I.2 that CdTe band gap was 1.6 eV at 5K, far from the Mn internal transition energy. The confinement, however, will increase the energy of the carriers in the quantum dot, getting them closer to the internal transition. To keep a strong enough luminescence, we then

have to be wary of the size of our studied dots in order to stay far enough from these Mn transitions.

^{6}A state of the Mn^{2+} is symmetric and thus almost not affected by the crystal field. However weakly, Mn^{2+} is still sensible to strain state at its position, leading to the Mn^{2+} strain induced fine structure. We can, in the equation, also take into account the hyperfine structure induced by the nuclear spin $I = \frac{5}{2}$ of the Mn atom. The Hamiltonian of the coupled electronic an nuclear spins of a Mn atom in a strained layer grow along [001] axis is known from electron paramagnetic resonance in CdTe/ZnTe superlattices [29] and reads:

$$\begin{aligned} \mathcal{H}_{Mn} &= \mathcal{A}\mathbf{I}.\mathbf{S} \\ &+\frac{1}{6}a(S_x^4 + S_y^4 + S_z^4 - \frac{1}{5}S(S+1)(3S^2+3S-1)) \\ &+D_0(S_z^2 - \frac{1}{3}S(S+1)) + E(S_y^2 - S_x^2) \end{aligned} \tag{I.98}$$

The first term is the hyperfine interaction between the Mn nuclear spin $\mathbf{I}$ and its $5d$ electrons spin $\mathbf{S}$, coupling two consecutive Mn spin states through an electron-nuclei flip flop. The hyperfine constant of the Mn was found to be $\mathcal{A} \approx 0.71$ μeV [30]. The second term results from the crystal cubic symmetry and mixes different S_z of the Mn spin. According to ref. [30], we have $a = 0.32$ μeV.

The last line contains terms linked to the strain state at the Mn position: the magnetic anisotropy caused by bi-axial strain D_0 and the anisotropy of strain in the xy plane E. D_0 is the dominant term for a Mn atom in a highly strained QD. Because of the partial relaxation of strain in the self-assembled QD we used, the value of D_0 may vary between 0 μeV for a strain-free QD, to 12 μeV for a fully strain CdTe layer matched on ZnTe. It splits the Mn spin states according to S_z^2 and is responsible for the Mn spin memory at zero magnetic field [31].

The anisotropy in the QD plane induces a mixing between different S_z through the anisotropic crystal field component E. It coupled two values of S_z separated by two units of spin. In the absence of magnetic anisotropy ($D_0 \simeq 0$), both the anisotropy of strain and the hyperfine structure prevent the optical pumping of the Mn spin at 0 magnetic field.

I.3.2 Cr atom in II-VI semiconductor

Cr atoms are incorporated into II-VI semiconductors as Cr^{2+} ions on cation sites forming a deep impurity level. This isotope presents *no nuclear spin*, meaning we don't have to consider the hyperfine structure of a Cr atom in a II-VI semiconductor. The ground state of a free Cr^{2+} is ^{5}D with the orbital quantum number $L = 2$ and a spin $S = 2$ yielding a 25-fold degeneracy. In the crystal field of T_d symmetry of the tetrahedral cation site in zinc-blende crystal, the degeneracy is

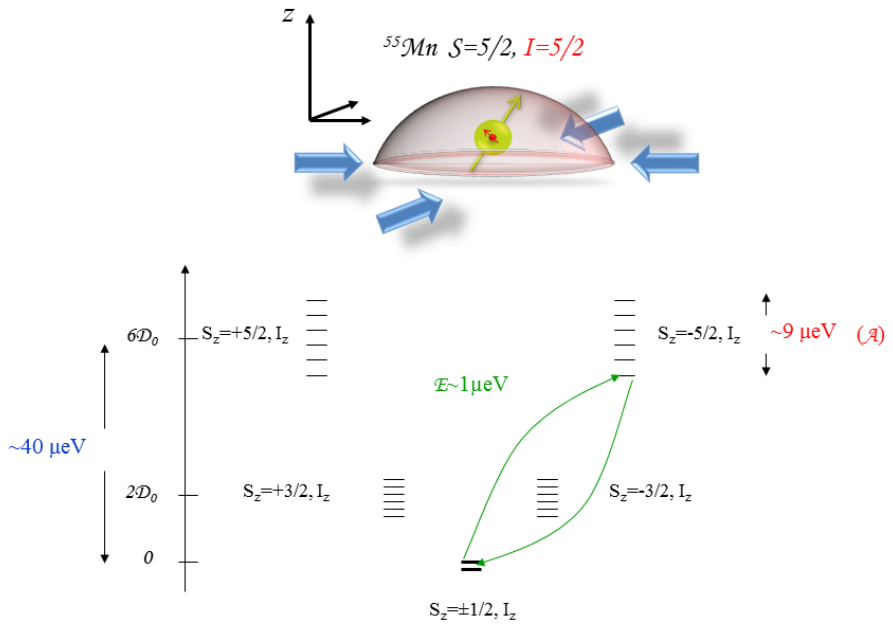

Figure I.8: Top: picture of an idealized strained QD containing a magnetic atom. Bottom: scheme of the energy level of a Mn atom in a strained II-VI QD. All the stable Mn isotopes ^{55}Mn carries a nuclear spin $I = \frac{5}{2}$ which couples through the hyperfine interaction ($\mathcal{A}\mathbf{I}.\mathbf{S}$) to the electronic spin $S = \frac{5}{2}$.The d orbital of the Mn is also sensitive to the electric field produced by the neighbouring crystal atoms (crystal field) in the zinc-blend lattice. A distortion of the lattice and consequently a change in the crystal field will also affect the d orbital. The dynamic of the Mn spin at zero magnetic field is mainly controlled by a magnetic anisotropy D_0 produced by the presence of a large bi-axial strain at the Mn location. This field splits the spin states of the Mn according to $D_0 S_z^2$; the anisotropy of the strain in the quantum dot plane ($E(S_y^2 - S_x^2)$) also mix the different S_z component (green arrow).

partially lifted (see Fig. I.3.2): the ^{5}D term splits into 15-fold degenerate orbital triplet ^{5}T$_2$ and 10-fold degenerate orbital doublet ^{5}E. The substitution of a Cd atom by a Cr atom lead to a Jahn-Teller distortion of the tetragonal matrix [32]. This distortion reduces the symmetry to D$_{2d}$ and leads to a splitting of the ^{5}T$_2$ ground state into a 5-fold degenerate ^{5}B$_2$ orbital singlet and a ^{5}E orbital doublet.

The ground state orbital singlet ^{5}B$_2$ is further split by the spin-orbit interaction. In a strain free crystal, it was found that the ground state splitting can be described

by the spin effective Hamiltonian [32]:

$$\mathcal{H}_{Cr,CF} = D_0 S_z^2 + \frac{1}{180} F[35S_z^2 - 30S(S+1)S_z^2 + 25S_z^2] + \frac{1}{6} a[S_1^4 + S_2^4 + S_3^4] \tag{I.99}$$

with the Cr spin $S = 2$ and $|D_0| \gg |a|, |F|$. In the model presented here, we use $a = 0$ and $F = 0$. The x, y, z principal axes were found to coincide with the cubic axes (1,2,3) giving rise to three identical sites, each given by I.99 but with the z axis of each along a different cubic axis (1,2,3). A value of $D_0 \approx +30$ μeV was estimated from Electron Paramagnetic Resonance (EPR) measurements in highly diluted bulk (Cd,Cr)Te [32].

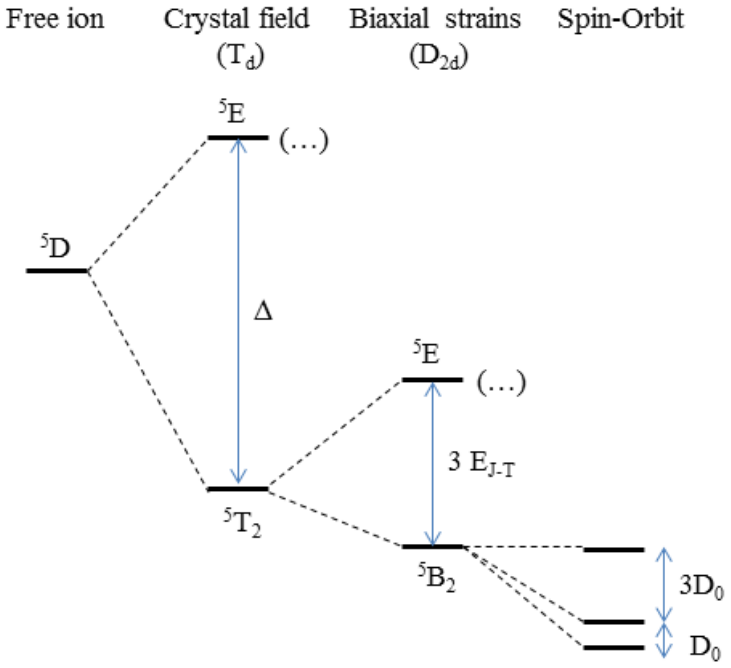

Figure I.9: Schema of the energy level splitting of Cr^{2+} at a cation site in II-VI compounds having zinc blende structure (T_d) with a crystal field parameter Δ, a Jahn-Teller energy E_{J-T} and a spin-orbit level spacing D_0.

Static biaxial compressive strain in the (001) plane, as observed in self-assembled quantum dots, reduces the symmetry to D_{2d} and destabilize the Cr $3d$ orbitals d_{xz} and d_{yz} having an electron density pointing along the [001] axis (z axis). The Cr ground state is then a 5-fold degenerated orbital singlet formed from the d_{xy} orbital. It corresponds to the Jahn-Teller ground state with a tetragonal distortion along the [001] axis [33].

An applied stress will also influence the Cr spin fine structure splitting through the modification of the crystal field and the spin-orbit interaction [32]. For an arbitrary strain tensor, the general form of the Cr ground state spin effective Hamiltonian is

$$\mathcal{H}_{Cr,\varepsilon} = c_1 e_A S_\theta + c_2 e_\theta S_\theta + c_3 e_\epsilon S_\epsilon + c_4 e_\zeta S_\zeta + c_5 (e_\xi S_\xi + e_\eta S_\eta) \tag{I.100}$$

with S_i defined as:

$$\begin{aligned} S_\theta &= S_z^2 - \frac{1}{2}[S_x^2 + S_y^2] \\ S_\epsilon &= \frac{1}{2}\sqrt{3}[S_x^2 - S_y^2] \\ S_\xi &= S_y S_z + S_z S_y \\ S_\eta &= S_x S_z + S_z S_x \\ S_\zeta &= S_x S_y + S_y S_x \end{aligned} \tag{I.101}$$

and e_i defined similarly as:

$$\begin{aligned} e_\theta &= \varepsilon_{zz} - \frac{1}{2}[\varepsilon_{xx} + \varepsilon_{yy}] \\ e_\epsilon &= \frac{1}{2}\sqrt{3}[\varepsilon_{xx} - \varepsilon_{yy}] \\ e_\xi &= \varepsilon_{yz} + \varepsilon_{zy} \\ e_\eta &= \varepsilon_{xz} + \varepsilon_{zx} \\ e_\zeta &= \varepsilon_{xy} + \varepsilon_{yx} \\ e_A &= \varepsilon_{xx} + \varepsilon_{yy} + \varepsilon_{zz} \end{aligned} \tag{I.102}$$

As shown in Sec. I.1.2, we can write for a flat self-assembled quantum dot with dominant large biaxial strain:

$$\begin{aligned} \varepsilon_{xx} &= \varepsilon_{yy} = \varepsilon_\parallel \\ \varepsilon_{zz} &= -2\frac{C_{11}}{C_{12}}\varepsilon_\parallel \end{aligned}$$

where $C_{11} \approx 5.4\ 10^{10}$ Pa and $C_{12} \approx 3.7\ 10^{10}$ Pa are the elastic constants of CdTe [34]. For this strain configuration, the Cr fine structure is controlled by the spin-lattice coupling coefficients c_1 (symmetric coefficient) and c_2 (tetragonal coefficients). Strain-coupling coefficients estimated from EPR measurements in bulk Cr doped CdTe are listed in table I.2.

We can now simplify the hamiltonian I.100, first reducing it to the active term in our case:

$$\mathcal{H}_{Cr,\varepsilon} = c_1 e_A S_\theta + c_2 e_\theta S_\theta$$

Table I.2: Values for spin to strain coupling coefficients of Cr in bulk CdTe (in meV) extracted from ref. [32].

c_1	c_2	c_3	c_4	c_5
-0.25±2	+4.9 ±2	-1.25±0.5	+4.9±2	+3.7±1.25

Replacing now e_A, e_θ and S_θ by their value given in I.101 and I.102, and using the equalities given in Sec. I.1.2, we can rewrite the strain controlled part of the spin Hamiltonian as $\mathcal{H}_{Cr,\varepsilon}$, depending only on $\varepsilon_\parallel$:

$$\begin{aligned} \mathcal{H}_{Cr,\varepsilon_\parallel} &= \underbrace{\frac{3}{2}\varepsilon_\parallel[2c_1(1-\frac{C_{12}}{C_{11}})-c_2(1+2\frac{C_{12}}{C_{11}})]}_{D_0} S_z^2 \\ &= D_0 S_z^2 \end{aligned} \tag{I.103}$$

where we can estimate $D_0 \approx 1\pm0.6$ meV from the values of the spin-strain coupling coefficients in CdTe (table I.2). However one should note the quantum dots could be partially relaxed and may contain a significant amount of Zn. We were not able to find spin to strain coupling coefficients for Cr in ZnTe and (Cd,Zn)Te alloy in literature. A value of $D_0 \approx +280$ μeV, much larger than for CdTe, was however estimated in strain-free Cr-doped bulk ZnTe [32]. Larger spin-strain coupling coefficients could than expected for Cr in ZnTe and (Cd,Zn)Te alloys.

Finally, an anisotropy of the strain in the quantum dot plane (001) with principal axis along [010] or [100] axes ($\varepsilon_{xx} \neq \varepsilon_{yy}$ and $\varepsilon_{xy} = \varepsilon_{yx} = 0$) would affect the Cr fine structure through the tetragonal coefficient c_3. This coupling can be described by an additional term in the spin-strain Hamiltonian

$$\begin{aligned} \mathcal{H}_{Cr,\varepsilon_\perp} &= \underbrace{\frac{3}{4}c_3(\varepsilon_{xx}-\varepsilon_{yy})}_{E} (S_y^2 - S_x^2) \\ &= E (S_y^2 - S_x^2) \end{aligned} \tag{I.104}$$

This anisotropy term E couples Cr spin states separated by two units and in particular S_z=+1 to S_z=-1 which are initially degenerated. It could be exploited to induce a large strain mediated coherent coupling between a mechanical oscillator and the Cr spin [35].

We can now group I.103 and I.104 in order to write the complete hamiltonian of an isolated Cr in a strained, anisotropic CdTe/ZnTe quantum dot:

$$\begin{aligned} \mathcal{H}_{Cr,\varepsilon} &= \mathcal{H}_{Cr,\varepsilon_\parallel} + \mathcal{H}_{Cr,\varepsilon_\perp} \\ &= D_0 S_z^2 + E(S_y^2 - S_x^2) \end{aligned} \tag{I.105}$$

I.4 A simple example: the X-Mn system

Lorem ipsum dolor sit amet, consectetur adipiscing elit. Curabitur tortor quam, imperdiet quis facilisis sed, fringilla a quam. Cras ante odio, hendrerit ac ante nec, cursus imperdiet urna. Mauris convallis ultricies purus, nec condimentum erat bibendum vel. Aliquam erat volutpat. Pellentesque condimentum, eros a consequat accumsan, turpis sem euismod nisi, sed fringilla quam turpis sit amet erat. Mauris dictum odio sed nisi dapibus, et molestie mauris rutrum. Praesent convallis dolor in nibh blandit bibendum. Quisque sit amet arcu consectetur lorem luctus venenatis nec quis dui. Aliquam erat volutpat. Aenean auctor elit nec tristique dignissim. Nulla massa mi, efficitur semper ex id, pretium eleifend massa. Vivamus sit amet orci scelerisque, gravida est ut, vulputate odio.

Figure I.10: QD spectra 0 Mn, 1 Mn, 2 Mn

Curabitur eget ipsum egestas dui viverra suscipit. Cras aliquet lacus vitae erat finibus semper. Nulla pharetra eget urna vitae sodales. Nunc faucibus velit lacus, nec ornare eros aliquet quis. Donec a orci nec sem pulvinar ultricies sit amet ut arcu. Nullam id vehicula enim, at tincidunt velit. Duis vestibulum lorem a molestie fringilla. Nullam tincidunt semper placerat. Donec nibh sem, ornare eget cursus ac, luctus sit amet eros. Phasellus eget interdum nisi. Donec mollis risus id lectus fringilla, et commodo risus iaculis. Donec at lacus sed nibh posuere posuere sit amet eget sapien. In dignissim, enim sit amet convallis fermentum, lacus nulla gravida tortor, non facilisis ex nisl sit amet augue. Maecenas eu enim condimentum, consectetur ligula vel, tincidunt nisl. Nam laoreet dictum volutpat. Donec at erat venenatis, ultrices lorem ac, vestibulum neque.

Figure I.11: Mn energy level in a QD

Bibliography

[1] J. K. Furdyna, "Diluted magnetic semiconductors", Journal of Applied Physics **64**, R29–R64 (1988).

[2] E. O. Kane, "Band structure of indium antimonide", Journal of Physics and Chemistry of Solids **1**, 249–261 (1957).

[3] C. Le Gall, "Dynamics and Optical contrôl of a single spin in a Quantum Dot", Theses (Université de Grenoble, Nov. 2011).

[4] J. M. Luttinger, "Quantum theory of cyclotron resonance in semiconductors: general theory", Phys. Rev. **102**, 1030–1041 (1956).

[5] G. Bir and G. Pikus, *Symmetry and strain-induced effects in semiconductors*, Wiley (1974).

[6] J. Allègre, B. Gil, J. Calatayud, and H. Mathieu, "Deformation potentials of cdte epilayers from piezo and wavelength modulation reflectivity spectra analysis", Journal of Crystal Growth **101**, 603–607 (1990).

[7] J. M. Luttinger and W. Kohn, "Motion of electrons and holes in perturbed periodic fields", Phys. Rev. **97**, 869–883 (1955).

[8] J.-L. Basdevant and J. Dalibart, "Mécanique quantique", in (Les éditions de l'École Polytechnique, 2002) Chap. 2, p. 80.

[9] W. Wardzyński and M. Suffczyński, "Dependence of the exchange splitting in excitons on the interatomic distance", Solid State Communications **10**, 417–419 (1972).

[10] M. Zieli ński, Y. Don, and D. Gershoni, "Atomistic theory of dark excitons in self-assembled quantum dots of reduced symmetry", Phys. Rev. B **91**, 085403 (2015).

[11] Y. Léger, "Détection de spins individuels dans les boîtes quantiques magnétiques", Theses (Université Joseph-Fourier - Grenoble I, Sept. 2007).

[12] C. L. Cao, L. Besombes, and J. Fernández-Rossier, "Spin-phonon coupling in single mn-doped cdte quantum dot", Phys. Rev. B **84**, 205305 (2011).

[13]Y. Léger, L. Besombes, L. Maingault, and H. Mariette, "Valence-band mixing in neutral, charged, and Mn-doped self-assembled quantum dots", Phys. Rev. B **76**, 045331 (2007).

[14]I. Favero, G. Cassabois, C. Voisin, C. Delalande, P. Roussignol, R. Ferreira, C. Couteau, J. P. Poizat, and J. M. Gérard, "Fast exciton spin relaxation in single quantum dots", Phys. Rev. B **71**, 233304 (2005).

[15]F. Patella, S. Nufris, F. Arciprete, M. Fanfoni, E. Placidi, A. Sgarlata, and A. Balzarotti, "Tracing the two- to three-dimensional transition in the inas/gaas(001) heteroepitaxial growth", Phys. Rev. B **67**, 205308 (2003).

[16]F. Tinjod, B. Gilles, S. Moehl, K. Kheng, and H. Mariette, "II–VI quantum dot formation induced by surface energy change of a strained layer", Applied Physics Letters **82**, 4340–4342 (2003).

[17]M. Bayer, G. Ortner, O. Stern, A. Kuther, A. A. Gorbunov, A. Forchel, P. Hawrylak, S. Fafard, K. Hinzer, T. L. Reinecke, S. N. Walck, J. P. Reithmaier, F. Klopf, and F. Schäfer, "Fine structure of neutral and charged excitons in self-assembled In(Ga)As/(Al)GaAs quantum dots", Phys. Rev. B **65**, 195315 (2002).

[18]C. Tonin, R. Hostein, V. Voliotis, R. Grousson, A. Lemaitre, and A. Martinez, "Polarization properties of excitonic qubits in single self-assembled quantum dots", Phys. Rev. B **85**, 155303 (2012).

[19]L. Maingault, "Insertion d'ions magnétiques dans les boîtes quantiques de semiconducteurs II-VI", Theses (Université Joseph-Fourier - Grenoble I, Dec. 2006).

[20]J. R. Schrieffer and P. A. Wolff, "Relation between the anderson and kondo hamiltonians", Phys. Rev. **149**, 491–492 (1966).

[21]J. Gaj, R. Planel, and G. Fishman, "Relation of magneto-optical properties of free excitons to spin alignment of mn^2+ ions in $cd_{1-x}mn_xte$", Solid State Communications **29**, 435–438 (1979).

[22]P. Kacman, "Spin interactions in diluted magnetic semiconductors and magnetic semiconductor structures", Semicond. Sci. Technol. **16**, R25 (2001).

[23]W. Mac, A. Twardowski, and M. Demianiuk, "S,p-d exchange interaction in Cr-based diluted magnetic semiconductors", Phys. Rev. B **54**, 5528–5535 (1996).

[24]J. Blinowski, P. Kacman, and K. Majewski, "Ferromagnetism in cr-based diluted magnetic semiconductors", Journal of Crystal Growth **159**, Proceedings of the seventh international conference on II-VI compouds and devices, 972–975 (1996).

[25]M. Herbich, W. Mac, A. Twardowski, K. Ando, Y. Shapira, and M. Demianiuk, "Magnetization and exciton spectroscopy of the diluted magnetic semiconductor $cd_{1-x}cr_xs$", Phys. Rev. B **58**, 1912–1921 (1998).

[26] Y. Tanabe and S. Sugano, "On the absorption spectra of complex ions. I", Journal of the Physical Society of Japan **9**, 753–766 (1954).

[27] D. McClure, "Solid states physics", in, Vol. 9 (Academics, New York, 1959).

[28] J. Griffith, *The theory of transition metal ions* (Cambridge University Press, London, 1971).

[29] M. Qazzaz, G. Yang, S. Xin, L. Montes, H. Luo, and J. Furdyna, "Electron paramagnetic resonance of mn2+ in strained-layer semiconductor superlattices", Solid State Communications **96**, 405–409 (1995).

[30] M. Causa, M. Tovar, S. Oseroff, R. Calvo, and W. Giriat, "Spin-lattice coefficients of mn2+ in ii–vi compounds", Physics Letters A **77**, 473–475 (1980).

[31] C. Le Gall, L. Besombes, H. Boukari, R. Kolodka, J. Cibert, and H. Mariette, "Optical spin orientation of a single manganese atom in a semiconductor quantum dot using quasiresonant photoexcitation", Phys. Rev. Lett. **102**, 127402 (2009).

[32] J. T. Vallin and G. D. Watkins, "EPR of Cr^{2+} in II-VI lattices", Phys. Rev. B **9**, 2051–2072 (1974).

[33] M. Brousseau, *Les defauts ponctuels dans les semiconducteurs* (Les Editions de Physiques, Sept. 1988).

[34] R. D. Greenough and S. B. Palmer, "The elastic constants and thermal expansion of single-crystal CdTe", Journal of Physics D: Applied Physics **6**, 587 (1973).

[35] P. Ovartchaiyapong, K. W. Lee, B. A. Myers, and A. C. B. Jayich, "Dynamic strain-mediated coupling of a single diamond spin to a mechanical resonator", Nature Communications **5**, 4429 (2014).